Advances in the chemistry and applications of alkali-metal–gas batteries

Advances in Chemistry and Application of Alkali Metal−Gas Batteries

Haining Gao[1] and Betar M. Gallant[2]*

[1]Department of Materials Science and Engineering, Massachusetts Institute of Technology, Cambridge, MA USA
[2]Department of Mechanical Engineering, Massachusetts Institute of Technology, Cambridge, MA USA
[*]e-mail: bgallant@mit.edu

Abstract | Rechargeable metal−gas batteries have received significant attention owing to the promise of exceeding the energy densities of Li-ion batteries. The prototype among this family has been the nonaqueous lithium−oxygen ($Li-O_2$) battery, which was developed with a vision of eventual application in electric vehicles. Significant challenges have, however, been identified with this battery, including parasitic chemical reactivity and degrees of electrochemical irreversibility, which have contributed along with other factors to poor charging and cycling. To address these issues, researchers began exploring new modes of nonaqueous metal−gas battery construction, which can be divided into three paths: Manipulation of the underlying O_2 redox behavior through electrolyte and materials design; Consideration of non-Li metal anodes to change the nature of the solid discharge phase and improve reversibility; and finally, consideration of other gas reactants as the cathode. This Review presents new scientific understanding of nonaqueous gas-to-solid electrochemistry that has emerged from these concerted efforts, along with new hurdles that have been revealed as cells have gradually been reformulated. The ultimate impact of new metal−gas batteries needs to be re-examined beyond that of only electric vehicles to carefully match strengths of individual chemistries and their varying performance characteristics with an expanded set of applications.

Introduction

The need for better rechargeable batteries to enable electric vehicles (EV) has been the main driver of battery research in past decades. Li-ion batteries, which have cell-level energy densities of 260 Wh/kg (700 Wh/L) and costs of $200−300/kWh, fall short of targets (350 Wh/kg, 750 Wh/L and <$125/kWh) deemed necessary for mass-market EV adoption.[1,2] Even with improvements, Li-ion batteries face physicochemical limits[3] inherent in how charge is stored: by bulk Li^+ insertion (intercalation), either into graphite at the anode or facilitated by transition-metal (Co, Ni, Mn) redox at the cathode. The cathode, such as $LiCoO_2$, $LiNi_xMn_yCo_{1-x-y}O_2$ (Li-NCM) or $LiNi_xCo_yAl_{1-x-y}O_2$ (NCA), is the capacity- and thus energy-limiting electrode in today's cells: transition metals have high weights but only store 1−2 electrons/metal, with capacities of 100−300 $mAh/g_{cathode}$ (500−1000 mAh/cc).[4]

Seeking pathways to higher energy, there has been an impetus to re-consider the nature of charge storage in batteries. Intercalation relies on lattice storage sites for Li^+ within a host phase; Li^+ shuttles into and out of materials with little volume expansion. As an alternative, conversion reactions—non-intercalation reactions that involve bulk phase transformations such as solid−solid, liquid−solid, or gas−solid— have received significant attention.[5-7] Conversion reactions are governed by physical phenomena distinct from intercalation reactions, including nucleation and growth of new phases, expressive volume change of electrodes, and unique and often more-complex reaction mechanisms. An example of an established conversion technology is the sulfur (S) cathode in Li−S batteries, which cycles by solid(−liquid)−solid transition between $S_8(s)$ and $Li_2S(s)$ during discharge and charge with high theoretical capacity (1672 mAh/g_{sulfur} or 1165 mAh/g_{Li_2S}, ~2.2 V vs. Li/Li^+).[8] Practical Li−S batteries have faced challenges including the formation of soluble polysulfides (reduced S intermediates, S_n^{2-}, n<8), which can create internal

shuttles between cathode and the Li anode during conversion to the final insoluble Li_2S end product, and are still maturing.[9] A second example is the transition metal fluoride class (MF_y, M = Fe, Co, Ni, Cu, y = 2 or 3) which cycle by the quasi-reversible reaction $MF_y + yLi \rightarrow M + yLiF$ with moderate voltages (~2.5−3.5 V) and high capacities (up to 700 $mAh/g_{cathode}$). Charging and cycling are limited by poor electrical contact and slow kinetics upon re-conversion of two phase-separated solids (M and LiF) back to MF_y upon charge, leading to large voltage hysteresis (> 1 V) and rate limitations.[5] Consequently, it became necessary to consider other cell chemistries in the search for high-energy batteries with potential to achieve good cycleability. This realization led to a sharp re-focusing on nonaqueous gas−solid—an alternative to solid−solid—electrochemistry around the beginning of the last decade (2010).

Batteries that employ gas cathodes and metal anodes have long been under development. Early efforts explored aqueous metal−air batteries (with zinc as the prominent anode candidate),[10] but had limited cycleability. Nonaqueous metal-liquified gas systems were also studied, with the Li−SO_2(l) battery as another prominent example,[11] but sustained reversibility was also elusive. The application viewpoint progressed in 1996, when K.M. Abraham and Z. Jiang reported the first rechargeable, nonaqueous lithium−oxygen (Li−O_2) battery. The cell used a polymer electrolyte and cobalt phthalocyanine-catalyzed carbon electrode, which facilitated discharge of O_2(g) to form solid lithium peroxide (Li_2O_2) at 2.5 V vs. Li/Li^+ (capacity of ~1600 mAh/g_{carbon}) and charged at 3.5−4 V vs. Li/Li^+.[12] It was later shown by Bruce and co-workers in 2006 that O_2(g) was evolved back on charge, confirming that electrochemical reversibility was indeed occurring.[13]

It was not until several additional studies on the use of solid catalysts,[14,15] which suggested the possibility of further lowering the charging voltage by several hundred millivolts, that the Li-O_2 field reached a tipping point and became one of the most hotly-researched battery topics in the

2010's, rapidly surpassing earlier metal-gas batteries.[7] Unfortunately, ensuing research led to a realization that intrinsic reactivity issues, involving O_2 redox in organic environments, prevent full electrochemical reversibility from being realized; today, commercially-viable charging voltages and cycle life have not yet been achieved.[16,17]

The challenges faced by Li−O_2 batteries, introduced in further detail below, led to great consternation but also newfound optimism in the prospect of developing novel battery chemistries with the capability to broaden today's energy and power portfolio. It is the aim of this Review to highlight recent scientific developments in the broadening field of nonaqueous alkali metal−gas batteries since emerging challenges began to dominate the Li−O_2 topic from around 2012−2013. To capitalize on successful aspects of Li−O_2, research pursuits diverged along three main paths. The first was a re-conception of the environment in which Li/O_2 redox occurs by changing either the electrolyte[20−22, 29−82] or the nature of oxygen electrochemistry itself.[83−93] A second path saw a willingness to turn away from Li anodes through investigation of alternative metals including sodium (Na),[94−108] potassium (K),[109−116] and others (**Fig. 1a**).[117,118] A third approach has been to reconceive the gas cathode entirely through exploration of new reactants, including oxide[11, 62, 119−144] and fluoride gases.[145−154] These efforts will be reviewed, and the placement of new nonaqueous metal−gas systems along the energy-reversibility axis will be examined. Together, this exploratory phase has led to a significant broadening of the combinatorial space for metal−gas battery design (**Fig. 1b**). Some high-energy systems have already been demonstrated at the laboratory scale. In other cases, attractive metrics have been proposed but not yet fully realized (**Fig. 1c**).

Metal-Gas Battery Principles

The Li−O_2 battery has served as an exemplar system through which understanding of gas-to-solid electrochemical reactions has significantly advanced. In the following, the cross-cutting operating principles of metal-gas batteries are briefly introduced using Li-O_2 as an example. During discharge, the principal reaction is:

$$\text{Anode} : 2Li(s) \leftrightarrow 2Li^+ + 2e^-$$

$$\text{Cathode} : O_2(g) + 2e^- + 2Li^+ \leftrightarrow Li_2O_2(s)$$

$$\text{Cell} : O_2(g) + 2Li(s) \leftrightarrow Li_2O_2(s) \quad (1)$$

$$E^o = 2.96 \text{ V vs. } Li/Li^+, Q_{theoretical} = 1168 \text{ mAh/g}, E_{theoretical} = 3457 \text{ Wh/kg}$$

Additional O_2-derived phases observed only occasionally in some cell configurations, such as lithium superoxide (LiO_2, 1 e^-/O_2) or lithium oxide (Li_2O, 4 e^-/O_2, E^o = 2.91 V vs. Li/Li^+), are discussed in a later section. In this review, following the field's convention and unless otherwise indicated, theoretical capacities and specific energies are based on total weight of gas and anode metal consumed to form the stoichiometric solid-phase product. As seen from the high capacity and energy of Reaction (1), the attraction of metal−gas batteries in general, and the Li−O_2 system in particular, is the switch from transition metal redox in Li-ion cathodes to molecular redox at the gas cathode, which significantly lessens cell weight per amount of charge stored.[18]

Practically, the cathode reaction proceeds on an electronically conductive surface, for example carbon, metals, conductive carbides or oxides,[16] which may also function as electrocatalysts to enhance kinetics of discharge and charge. The reactant gas is introduced in the cell headspace and dissolved locally within the electrolyte in accordance with Henry's Law; typical solubilities are ~1-10 mM for O_2(g) at atmospheric pressure in nonaqueous electrolytes.[19,20] Upon discharge, the solid phase nucleates and grows on the electrode surface and within the pore

structure of the cathode. The nucleation and growth modes of solid alkali phases are highly sensitive to electrolyte in general, along with electrode material and discharge rate/overpotential (degree of deviation of actual voltage from the thermodynamic voltage), and can result in morphologies ranging from discrete particles to coatings.[21-23] Theoretical capacities, as in Reaction (1), omit the weight of the cathode substrate, which is determined by engineering considerations and can vary. An optimized electrode structure presents high surface areas for electrochemical reactions, high pore volumes to accommodate growth of the solid phase, and minimum substrate weight.[24] With judicious cathode architecting, close-to-theoretical capacities and energy densities have been experimentally demonstrated in Li-O_2 batteries.[18] As many studies continue to focus on the underlying electrochemistry given fundamental challenges (described further herein), capacities are reported by normalizing to the weight of the substrate (usually carbon) for simplicity.

It was originally proposed that metal-O_2 batteries could obtain O_2 for "free" from air, and thus the weight of O_2 was omitted in early energy estimates. (Note that the reaction to form Li_3N from N_2, at $E^o = 0.44$ V,[25] is too low to be assessable at typical gas cathodes).[26] It is now understood that a supply of pure O_2 is required given sensitivity of alkali metal−O_2 electrochemistry to water.[27] The weight of the gas cylinder and additional balance-of-plant is not included in theoretical calculations but will further deduct from specific and volumetric energies.[28] Given that more immediate reactivity and underlying chemical issues are still pervasive, development of alkali metal-gas technology has not progressed substantially to a prototyping phase. In the following, the electrochemical mechanisms of Li-O_2 batteries are elaborated in greater detail before progressing to emerging chemistries.

Li−O_2 batteries: Electrochemical mechanisms

Early studies on Li-O_2 batteries utilized electrolytes containing organic carbonate solvents (such as propylene carbonate or ethylene carbonate/dimethyl carbonate), which were directly translated from Li-ion technology. Carbonate solvents, however, were later found to readily degrade in the presence of O_2 discharge intermediates. This reactivity led to formation of lithium carbonate (Li_2CO_3) rather than Li_2O_2, making the cell electrochemically irreversible (CO_2, rather than O_2, is released upon charge).[29-31] Consequently, non-carbonate solvents such as ethers (glymes, tetrahydrofuran–THF) or dimethylsulfoxide (DMSO), among others, are nowadays utilized. In the search for viable, less-reactive solvents, it became clear that the electrolyte has a significant role to play in guiding the pathways of O_2 reactivity.

The role of the electrolyte on discharge reaction path and rechargeability. In non-carbonate solvents, O_2 reduction follows a step-wise reaction pathway that is strongly governed by solvent chemistry due to variable solubility of the principal discharge intermediate, superoxide (O_2^-), in different environments.[21,32] O_2 reduction branches between surface- or solution-localized processes (* indicates a surface state, 'sol' denotes dissolved species):

Surface reaction (cathode):

$$O_2(g) + e^- + Li^+ \rightarrow LiO_2^* \quad (E) \tag{2}$$

$$LiO_2^* + e^- + Li^+ \rightarrow Li_2O_2^*(s) \quad (E) \tag{2a}$$

$$2LiO_2^* \rightarrow Li_2O_2^*(s) + O_2(g) \quad (C) \tag{2b}$$

Solution reaction (cathode):

$$O_2(g) + e^- + Li^+ \rightarrow Li^+ O_2^-(sol) \quad (E) \tag{3}$$

$$Li^+ O_2^-(sol) + e^- + Li^+ \rightarrow Li_2O_2(s) \quad (E) \tag{3a}$$

$$2(Li^+ O_2^-(sol)) \rightarrow Li_2O_2(s) + O_2(g) \quad (C) \tag{3b}$$

(E) denotes an electrochemical step whereas (C) denotes a chemical disproportionation step of two LiO_2 to form $Li_2O_2(s) + O_2(g)$. Evidence that the reaction pathways proceed through the O_2^-/LiO_2 intermediate was provided by shell-isolated nanoparticle enhanced Raman spectroscopy and surface-enhanced Raman spectroscopy, which detected adsorbed O_2^- on reacting electrodes.[21,33-35] Selectivity between solution and surface pathways is determined by availability of Li^+ to react with O_2^- (**Fig. 2a**). Larger Li^+ desolvation barriers (or stronger superoxide-solvent interactions) impede association of Li^+ and O_2^-, supporting higher O_2^- diffusivity farther from the cathode before LiO_2 and subsequently Li_2O_2 are formed. Solution-phase growth supports gentler precipitation of Li_2O_2 on existing Li_2O_2 nuclei, favoring large 'toroid'-shaped particles (hundreds of nm to μm scale, **Fig 2b**), rather than on the electrode substrate which instead supports film-like growth. Promotion of larger Li_2O_2 particles retains the cathode's surface clear for continued reaction, extending the maximum capacities which are determined by the eventual passivation of the electrode surface.[36,37] Electrolyte factors that decrease Li^+ activity and promote solution-mediated growth are several-fold. These include high Guttman donor number (DN) solvents, which lower the Lewis acidity of the cation through strong solvation (for example, DMSO);[21,38] high anion acceptor number / ionic strength, which determines coordination strength with Li^+ and modulates Li^+ availability for reaction with O_2^-;[39] the presence of solubilizing additives that engineer enhanced O_2^- solubility into the bulk electrolyte, for example H_2O;[40,41] and/or the utilization of discharge redox mediators (RM) to generate soluble complexes with reduced oxygen intermediates, which shuttle reduced oxygen through the electrolyte to Li_2O_2 nuclei, where they react with Li^+ and contribute to particle growth. Examples of discharge RM include 2,5-di-tert-butyl-1,4-benzoquinone (DBBQ),[42,43] combined DBBQ+H_2O,[44] phenol,[45,46] vitamin K2,[47] and coenzyme Q_{10}[48] among many others.[49] Meanwhile, high solvent Acceptor Numbers likewise decrease O_2^- reactivity, with similar outcomes regarding

Li_2O_2 particle size and capacity.[40] In addition to solvent properties, discharge rate (production rate of O_2^-) will also determine the rates of supersaturation of electrolyte with O_2^- and of Li_2O_2 precipitation,[50] and can likewise distinguish between solution (lower rate) and surface (higher rate) mechanisms within a given solvent.[40] Exceedingly high capacities have been achieved through electrolyte engineering (areal capacities >15 mAh/cm^2).[17] Multiple reviews have elsewhere summarized electrolyte, discharge redox mediator and material parameters that modulate the discharge behavior of Li−O_2 batteries to obtain high capacities, to which the reader is referred for additional details. [16,18,32,49,51-53]

Unfortunately, oxygen reduction intermediates and products generated on discharge parasitically react with many cell components including electrolyte,[54,55] carbon,[56] and binder.[57] Problematic species include strongly nucleophilic and basic O_2^-/LiO_2 and Li_2O_2.[58] It was later found that highly reactive singlet oxygen ($^1O_2$) forms during disproportionation (Reactions 2b and 3b) and rapidly degrades organic solvents;[59] $^1O_2$ has been proposed to account for a majority of side products formed.[60,61] (Superoxide and $^1O_2$ are likewise generated during the charging reactions).[62] Consequently, quantities of parasitic solid products, including lithium- and alkyl carbonates, are found to varying extent with nearly all electrolytes and accumulate over cycling.[63] Critically, when O_2^- solubility is promoted, side reactions can become amplified in the same systems (such as high DN) that promote high capacities and best performance.[64] More drastically, reversibility of Li_2O_2 back to O_2 and Li on charge remains hindered by impractically high charging voltages of approximately 4 V vs. Li/Li$^+$ and above (**Fig. 2c**). The high charging voltages arise from the resistive nature of parasitic products,[65] the insulating Li_2O_2 phase itself (bandgap of >5 eV for stoichiometric Li_2O_2),[57] and possible intrinsic kinetic limitations of Li_2O_2 oxidation, which are still being elucidated.[18,55,66]

Some strategies have been proposed to address chemical irreversibilities. These include use of non-carbon electrodes, such as gold,[67] conductive carbides such as TiC,[68,69] or oxides such as Ti_4O_7,[70] with increased oxidative stability to minimize corrosion and side-product formation;[67,68] solid catalysts to attempt to decrease charging voltages;[51] and reliance upon electrolyte-soluble redox mediators which can also facilitate Li_2O_2 decomposition on charge.[71-73] The role of solid catalysts in lowering charging voltages has been debated;[31,74,75] it is challenging to disentangle the catalyst's effect on Li_2O_2 discharge morphology and possible role in promoting other side-reactions, making it difficult to unambiguously prove whether solid catalysts function as intended. Soluble charge redox mediators, such as tetrathiafulvalene, lithium iodide (LiI), and lithium bromide (LiBr)[76] are highly effective at enabling charge at lower voltages (~3.3−3.6 V vs. Li/Li^+).[71,77] Charge RM function as chemical oxidants for Li_2O_2, in which the RM is charged ($RM \rightarrow RM^+ + e^-$) rather than the Li_2O_2 directly; the soluble RM^+, which must have a redox potential >2.96 V vs. Li/Li^+ to oxidize Li_2O_2, diffuses to Li_2O_2 and chemically charges it, converting back to RM. This process shifts the redox process away from the substrate/Li_2O_2 interface to the Li_2O_2/electrolyte interface, and can effectively decompose large amounts of Li_2O_2 at potentials pinned by the potential of the charge RM. Charge RMs have also been reported to effectively oxidize other phases: using LiI and a reduced graphene oxide cathode in 1,2-dimethoxyethane (DME) electrolyte with various amounts of added water, lithium hydroxide (LiOH), rather than Li_2O_2, was the major product and could be successfully decomposed by LiI around ~3 V vs. Li/Li^+.[78] LiI was later found to be the source of the unanticipated LiOH formation.[79] Regardless of product, a major challenge in use of charge RM is their high solubility within the electrolyte and tendency to shuttle to the anode, where they can react with Li. Charge RMs are also susceptible to reaction with $^1O_2$.[80] A third challenge is incomplete O_2 recovery, which is compared

stoichiometrically with the amount of Li_2O_2 formed on discharge, and tends to be below 95%.[17] Finally, there is no clear indication of end-of-charge with charge RMs, such as the characteristic voltage uptick commonly observed with completion of direct Li_2O_2 oxidation (**Fig. 2c**). Consequently, it is uncertain whether charge RMs have a future in real cells. Overall, the practicality of engineering approaches (non-carbon electrodes, solid and soluble catalysts) from a weight, cost, and cell-level perspective remain uncertain, and in many instances introduce significant complexity into the cell.

Even if cathode reactivity issues could be solved, strategies that realize high energies on discharge rely on low rates to promote large Li_2O_2 toroids; the Li−O_2 battery has poor rate capability at even moderate powers, with significant losses in attainable voltage and capacity occurring as rate increases. The latter is traceable to the formation of smaller particles and more rapid passivation. In addition, large Li_2O_2 toroids require higher charging overpotentials than smaller coatings of Li_2O_2 particles, which retain closer electronic contact with the substrate.[37] Thus, a fundamental tension of the topic lies between high specific energy density on the one hand – favoring formation of large toroids with high void-volume filling – and reversibility on the other.[54] A final challenge pertains to Li anodes, which face cycleability challenges at even moderate rates due to parasitic reactivity with the electrolyte,[81] and may require protection strategies to block parasitic reactivity with O_2 and oxygen intermediates,[82] and/or oversizing to provide an extra reservoir for long-term cycling. Such efforts are however outside the scope of this Review given that cathode reversibility has yet to be fully demonstrated.

Li−"O" batteries: Beyond conventional O_2 reactions. The above challenges spurred researchers to re-evaluate the fundamental nature of oxygen redox in Li batteries. One option to avoid high charge voltages associated with Li_2O_2 decomposition is to block full reduction of O_2 to

Li_2O_2 upon discharge. Lopez and co-workers reported a proof-of-concept of using the electrolyte as the storage phase for the peroxide dianion (O_2^{2-}) through complexation with hexacarboxamide cryptand during discharge, leading to reversible cycling of $O_2 \rightleftharpoons O_2^{2-}$ in the presence of tetrabutylammonium perchlorate ($TBAClO_4$) in THF.[83] However, cryptand concentrations were <10 mM and practical performance with alkali salts have yet to be demonstrated. Researchers also reported that certain electrode materials, such as iridium (Ir) supported on reduced graphene oxide (rGO), can promote surface stabilization of LiO_2 rather than Li_2O_2, which yielded improved reversibility with charging voltages <3.5 V vs. Li/Li^+ (**Fig. 2b,c**).[84] There has been debate about whether LiO_2 can truly be stabilized,[85] as Raman shifts relied upon to identify LiO_2 exhibit overlap with binder degradation peaks,[86] and some researchers found only Li_2O_2 as the discharge product on Ir-rGO.[86] The ability of nanoscale materials to promote bulk LiO_2 formation at practical quantities remains uncertain, while the chemical reactivity of LiO_2 with conventional electrolytes remains an issue for cell lifetime.

A second approach to tackle the reactivity of reduced oxygen species is to move away from organic electrolytes in favor of less-reactive electrolyte environments. Molten salt electrolytes ($LiNO_3$–KNO_3–$CsNO_3$ eutectics) have been successfully used in Li–O_2(g) batteries with operation above the liquidus point (ca. 150 °C).[87] Significantly higher capacities (~1300 mAh/g_C) were obtained compared to $LiClO_4$/DMSO (~900 mAh/g_C), and were attributed to enhanced solubility of LiO_2/Li_2O_2 during discharge in the molten environment; improved kinetics with dramatically lowered charging overpotentials (~50 mV at 80 mA/g_C) on carbon were observed. Building upon this concept, it was reported that Ni acts as an active catalyst for O_2 reduction and evolution in molten nitrate salt and can enable reversible, 4-electron reduction of O_2 to Li_2O at 150 °C, where Li_2O becomes thermodynamically favored over Li_2O_2.[88] Very high areal capacities (11

mAh/cm^2) and charging below 3 V vs. Li/Li$^+$ (**Fig. 2c**) were achieved at low rates (0.1 mA/cm^2, based off the geometric area), with 150 reversible cycles.

Recently, researchers discovered that gaseous O_2 is not required as the electroactive oxygen source in these molten nitrate electrolytes. Using Ni nanoparticle catalysts and without any O_2 introduced in the cell, NO_3^- anions were reversibly reduced to NO_2^- in KNO_3–$LiNO_3$ eutectic, forming Li_2O:[89]

$$\text{Anode: } 2Li(s) \leftrightarrow 2Li^+ + 2e^-$$

$$\text{Cathode: } LiNO_3(l) + 2e^- + 2Li^+ \leftrightarrow Li_2O(s) + LiNO_2(l)$$

$$\text{Cell: } 2Li(s) + LiNO_3(l) \leftrightarrow Li_2O(s) + LiNO_2(l) \quad (4)$$

$$E^o = 2.44 \text{ V vs. Li/Li}^+, Q_{theoretical} = 647 \text{ mAh/g}, E_{theoretical} = 1579 \text{ Wh/kg}$$

The theoretical specific energy of this system includes the weight of the consumed nitrate and Li. At 150 °C and 0.1 mA/cm^2, the authors reported comparably high areal capacities (~12 mAh/cm^2) to the related system with O_2(g).[88] Charging occurred at ~2.55 V vs. Li/Li$^+$. This work showed for the first time that bulk electrolytes can function as reversible storage reservoirs for O in the NO_3^-/NO_2^- couple, freeing restrictions of carrying an O_2 supply while successfully achieving high-reversibility pathways. However, the requirement to operate at elevated temperature may limit usage to specialty applications at first, such as military or space, rather than EVs as was originally imagined for the Li–O_2 battery, at least until compatibility with vehicle designs and system engineering challenges can be addressed.

A third approach considered oxygen redox confined entirely to the solid phase. Nanolithia (Li_2O)–$LiCoO_2$ composites, beginning with O in the fully reduced state, was shown capable of oxidation up to mixed LiO_2/Li_2O_2, thus can also be considered as a Li-ion battery cathode with

anionic redox.[90,91] Subsequent reversible cycling was possible even when using carbonate electrolyte (ethylene carbonate / diethyl carbonate).[92] The cell reactions (indicated on charge) are:

$$\text{Anode: } 2Li^+ + 2e^- \leftrightarrow 2Li(s)$$

$$\text{Cathode: } 2Li_2O \leftrightarrow 2e^- + 2Li^+ + Li_2O_2(s)$$

$$\text{Cell: } 2Li_2O \leftrightarrow 2Li + Li_2O_2(s) \quad (5a)$$

$$E^o = 2.86 \text{ V vs. } Li/Li^+, Q_{theoretical} = 897 \text{ mAh/g}, E_{theoretical} = 2565 \text{ Wh/kg}$$

$$\text{Anode: } 3Li^+ + 3e^- \leftrightarrow 3Li(s)$$

$$\text{Cathode: } 2Li_2O \leftrightarrow 3e^- + 3Li^+ + LiO_2(s)$$

$$\text{Cell: } 2Li_2O \leftrightarrow 3Li + LiO_2(s) \quad (5b)$$

$$E^o = 2.88 \text{ V vs. } Li/Li^+, Q_{theoretical} = 1341 \text{ mAh/g}, E_{theoretical} = 3862 \text{ Wh/kg}$$

The practical discharge voltage of ~2.55 V vs. Li/Li^+ is slightly lower than in liquid Li−O_2 systems (~2.7 V vs. Li/Li^+); charge voltages were close to the theoretical values (**Fig. 2d**). Reversible cycling up to ~200 cycles was reported with a charge capacity cutoff of 615 mAh/g, approximately half of the theoretical maximum of the Li_2O/LiO_2 couple. However, reactivity between O_2^- and electrolyte resulted in a shuttle phenomenon of organic species in the electrolyte. To improve cyclability, other researchers utilized an alternative catalytic matrix of Ir/reduced-graphene oxide as the scaffold for Li_2O, aiming to combine and stabilize the active Li-deficient intermediate state.[93] Up to 2,000 cycles with 99.5% Coulombic Efficiency (electrical charge obtained from solid phase oxidation compared to that consumed during discharge) were reported in Li cells with capacity of 400 $mAh/g_{cathode}$. While promising, this capacity is significantly lower than the theoretical capacity of Li_2O_2 (1168 mAh/g), and thus reversibility is gained at the expense of both specific energy and cost.

Efforts to explore novel O redox have been scientifically fruitful and achieved significant improvements in cell reversibility at the laboratory scale. However, redefining the electrochemistry at the heart of the battery has also introduced new challenges in the required cell operating temperatures, chemical reversibility, reliance on precious metals, and/or overall practicality that point towards adjusted expectations for applications and mass-market suitability of this technology.

Alternative metal anodes

Facing these challenges, researchers began to explore new options to modify the electrochemistry by replacing the Li anode. Early progress in terms of reversibility was most apparent with Na and K. Unlike Li, which does not form a stable superoxide and instead disproportionates to Li_2O_2, the larger alkali cations (and softer Lewis acids) facilitate stable superoxides, which are the dominant discharge phase. Fortuitously, alkali superoxide phases have also been shown to have improved reversibility.

Na−O₂. In 2012, Hartmann and co−workers[94] reported that dramatic improvements in O_2 redox reversibility could be achieved by changing the alkali metal from Li to Na. Discharge voltages were lower, at ~2.2 V vs. Na/Na^+, given the modified thermodynamics, and charge voltages were ~2.3 V vs. Na/Na^+ (at 120 μA/cm^2) in an ether electrolyte (diethylene glycol dimethyl ether), representing an astonishing degree of voltage reversibility previously not observed in a metal−O_2 system. The round-trip Coulombic Efficiency was ~90% (**Fig. 3**).

Although the discharge product, sodium peroxide (Na_2O_2), is slightly more thermodynamically favourable (E^o = 2.33 V vs. Na/Na^+), the one-electron reduction product sodium superoxide (NaO_2, E^o = 2.27 V vs. Na/Na^+) was found to comprise the majority discharge phase experimentally. This was proposed to occur because the one-electron reduction is kinetically

preferred compared to the two-electron reaction to peroxide.[94] The discharge reaction is therefore (**Fig. 3a**):

$$\text{Anode : } Na(s) \leftrightarrow Na^+ + e^-$$

$$\text{Cathode : } O_2(g) + e^- + Na^+ \leftrightarrow NaO_2(s)$$

$$\text{Cell : } O_2(g) + Na(s) \leftrightarrow NaO_2(s) \quad (6)$$

$$E^o = 2.27 \text{ V vs. } Na/Na^+,\ Q_{theoretical} = 487 \text{ mAh/g},\ E_{theoretical} = 1108 \text{ Wh/kg}$$

The specific energy of the Na system is significantly lower than Li−O_2 (**Fig. 1c**) given the higher weight of Na along with lower cell voltages. NaO_2 forms as cubic deposits with characteristic sizes much larger than that of Li_2O_2 (>10 μm *vs.* <1 μm, **Fig. 3b**), implying that higher volumetric fillings and thus energy densities might be attained. The large cubic particles have been attributed to a solution-phase mechanism by which NaO_2 chemically precipitates from the supersaturated electrolyte, a mechanism that is also invoked in reverse to allow the large, electronically insulating particles to decompose upon charge.[95] Protons, sourced from water even at trace quantities (10 ppm) in the electrolyte, were later implicated as the phase-transfer catalyst that promotes shuttling of superoxide by hydroperoxyl radicals (HO_2) to precipitate as NaO_2 onto active nuclei.[96,97]

The single-electron nature of the O_2/NaO_2 couple, compared to two electrons transferred between O_2/Li_2O_2, was also suggested to underlie improved kinetics on charge.[94] In addition, the solid superoxide phases exhibit shorter O-O bond distances in the solid phase (1.28 – 1.34 Å, closer to the O-O bond of O_2(*g*) at 1.208 Å than in the peroxides, **Table 1**) which facilitates facile O_2 evolution. Improved charging overpotentials in Na−O_2 compared to Li−O_2 were also attributed to lower reactivity of NaO_2 towards the electrolyte, avoiding formation of deleterious Na_2CO_3 which requires high voltages to decompose.[98]

There has been significant discrepancy about the exact nature and stability of discharge products. In subsequent work, some studies suggested the formation of other products aside from NaO_2, such as Na_2O_2 and $Na_2O_2{\cdot}2H_2O$, as summarized in Ref.99 Further analyses continue to support the observation of NaO_2 as the primary discharge product under typical cell operating conditions.[100,101] It was found that NaO_2 chemically reacts upon cell rest (without active current flowing), releasing O_2^-, which converts to HO_2 by solvent proton extraction and ultimately forms $Na_2O_2{\cdot}2H_2O$, providing a possible answer for this controversy.[102] Other studies have also concluded that cell resting is highly detrimental for cell reversibility.[103] This points to an inherent challenge with forming NaO_2 as the discharge phase, in spite of intrinsically improved reversibility achievable under dynamic conditions.

As development of Na−O_2 batteries progressed, subsequently-discovered challenges were found to be several-fold:[104,105] Incomplete reversibility upon charge and, relatedly, limited cycle life (tens of cycles before drastic capacity loss); Pore-clogging due to excessive NaO_2 accumulation nearest the O_2 reservoir, limiting O_2 transport within the porous electrode and attainable capacities;[106] Aforementioned electrolyte side reactions at the cathode including gradual reactivity and conversion of NaO_2;[107] Issues related to the Na anode, including dendrite formation and excessive reactivity with the electrolyte salt,[108] which may also necessitate Na protection strategies in future development. It remains to be seen whether the intrinsic chemical reactivity issues of Na−O_2 will be solved to an extent needed for this cell technology to succeed, even if other issues can be addressed.

K−O₂. In 2013, an alternative pathway was opened for development of O_2 cathodes by the demonstration of the first potassium−oxygen (K−O_2) cell.[109] The formation of potassium superoxide (KO_2, E^o = 2.48 V vs. K/K^+) is both thermodynamically and kinetically more

favourable than that of potassium peroxide (K_2O_2, E^o = 2.20 V vs. K/K^+) and potassium oxide (K_2O, E^o = 1.67 V vs. K/K^+). This is consistent with experiments, where KO_2 was found to be the solitary discharge product, with cubic morphology in ether electrolytes (solution-mediated pathway) or dendritic structure in DMSO electrolyte (surface-mediated pathway).[110,111] The overall cell reactions are:

$$\text{Anode} : K(s) \leftrightarrow K^+ + e^-$$

$$\text{Cathode} : O_2(g) + e^- + K^+ \leftrightarrow KO_2(s)$$

$$\text{Cell} : O_2(g) + K(s) \leftrightarrow KO_2(s) \quad (7)$$

$$E^o = 2.48 \text{ vs. } K/K^+,\ Q_{theoretical} = 377 \text{ mAh/g},\ E_{theoretical} = 935 \text{ Wh/kg}$$

While the corresponding theoretical specific energy is yet lower given the lower theoretical capacity of KO_2 (**Fig. 1c**), the discharge voltages are slightly higher than that of Na−O_2. In addition, a charge/discharge voltage hysteresis of <50 mV was observed at areal currents of 160 μA/cm^2 with charge efficiencies of ~90% (**Fig. 3c**), with reversibility roughly on par with that of Na−O_2, making the system intriguing for further study.

The larger size of K^+ was, compared with Li^+ and Na^+, found to be advantageous for stability of the superoxide phase due to reduced Lewis acidity. The recurring challenge of superoxide reactivity with the electrolyte was, however, noted even in the first study,[109] though it was later shown that KO_2 discharge products exhibit improved stability upon aging in discharged cells (94% Coulombic Efficiency on charge retained after aging in the discharged state for 30 days at rest) and are thus much less reactive than the NaO_2 counterpart.[112] The K−O_2 system has been found to be the only one that does not produce $^1O_2$ during charge/discharge, making it distinct from Li−O_2 and Na−O_2 systems and potentially more stable.[61]

In spite of attractive first-cycle performance, enhanced reactivity of the K metal anode became a major hurdle for this battery as the anode is generally found to limit the cycle life of cells. O_2 crossover and reactivity are particularly problematic for K, leading to anode passivation by KO_2 along with KOH, K_2CO_3, and other organic decomposition products in ethers. To address this, some strategies focused on K anode protection, including use of K^+- conducting artificial interfaces.[113] These solutions will add additional weight to the cell, further decreasing the specific energy density. Use of electrolyte strategies to form a protective layer on K were reported using $KNTf_2$ (Tf = CF_3SO_2) salt in ethers, extending the cycle life to >60.[114] A recent study found that operation in dry air, rather than pure O_2, is beneficial as the lower partial-pressure of O_2 directly addresses the anode reactivity issue; up to 100 cycles with 99% Coulombic Efficiency were achieved.[115] Ambient air-operation was not, however, beneficial as the reactivity of KO_2 with H_2O and CO_2 leads to aggressive formation of $KHCO_3$. A promising strategy may be to remove K metal entirely; another recent study reported that a potassium biphenyl organic anode could be used as a successful couple to a KO_2 cathode, achieving 3000 cycles with >99% Coulombic Efficiency, a dramatic new benchmark for this system.[116] The cell specific and volumetric energies will, however, be further lowered in this system. Overall, continued improvements in performance metrics are needed to demonstrate the commercial feasibility of $K–O_2$ batteries; regardless, exploration of this system has been highly scientifically valuable to gain new insights into O_2 electrochemistry and product reversibility.

Additional metals. In the course of exploring alternative anode metals as possible nonaqueous couples with O_2, it should be noted that other anodes were tried, including magnesium (Mg),[117] and calcium (Ca)[118] with variable theoretical metrics. These metal anodes suffer additional stability, reversibility, and electrolyte requirements than the alkali metals reviewed

herein, and are less of a "drop-in" technology, requiring more dramatic re-design of the cell. They are thus outside the scope of this review; we refer the reader to the individual citations for additional details.

Overall, the numerous challenges with oxygen conversion cathodes led some researchers, including the authors, to further consider an alternative approach to inject new life into the metal−gas topic: retaining the Li anode, but doing away with O_2 as the gas cathode entirely.

'Beyond O_2' gas cathodes

An alternative approach to address the challenges in Li−O_2 batteries is to drastically change the reaction chemistry by considering novel gas-to-solid cathodes for coupling with Li (**Fig. 4**). As with Li−O_2, the attraction of such chemistries lies in the avoidance of transition-metal-based redox and the use of Li anodes, and thus high theoretical specific energies (**Fig. 1c**). Such 'beyond-O_2' cathodes can be roughly divided into two categories: Oxide gases, aiming to achieve cyclability with high specific energy (for example SO_2) or to broaden the functionality of battery systems entirely to span new applications for environmental cleanup (for example CO_2); or fluoride gases, which have unique potential for ultrahigh-energy for portable power applications. Given the earlier-stage nature of these new systems, performance metrics can be considered preliminary, without intensive efforts expended yet in most cases to develop battery prototypes.

Li−SO_2. The primary Li−SO_2 battery was first developed in the 1960s,[11] and found commercial success in military and aerospace due to its long shelf life, good rate performance and wide operating temperature window (-40 to 55 °C).[119] Typical electrolytes consist of compressed, liquefied SO_2 (>3.4 atm) and an organic solvent (typically acetonitrile) or ionic liquid.[120] The cell reaction is:

$$\text{Anode} : 2Li(s) \leftrightarrow 2Li^{+} + 2e^{-}$$

$$\text{Cathode}: 2SO_2(l) + 2e^- + 2Li^+ \rightarrow Li_2S_2O_4(s)$$

$$\text{Cell}: 2SO_2(l) + 2Li(s) \rightarrow Li_2S_2O_4(s) \quad (8)$$

$$E^o = 3.0 \text{ V vs. } Li/Li^+, Q_{theoretical} = 378 \text{ mAh/g}, E_{theoretical} = 1133 \text{ Wh/kg}$$

Note that the relatively lower specific energy compared to Li-O_2 arises from the added weight of sulfur and incomplete utilization of O for charge storage. Limited rechargeability (<15 cycles) of this system was first indicated by Maricle and Mohns in 1971.[121] At that time, it was believed that the reaction forming insoluble $Li_2S_2O_4$ was irreversible. In the following two decades, the rechargeability of the Li−SO_2(*l*) system was improved through alternative reaction pathways (such as those involving participation of the electrolyte salt), instead of Reaction 8. For example, $LiAlCl_4$ salt was shown to form a complex with SO_2 and carbon, thus the reduction products became LiCl and $LiClAl(OSO\text{-}C)_3$, which had a better reversibility (50 cycles).[122] Despite efforts made to identify optimized salts by using alternatives such as $Li_2B_{10}Cl_{10}$ or $LiGaCl_4$, early rechargeable SO_2(*l*) prototypes still suffered from Li stability issues and limited cycles.[123] It was not until recently that the Li−SO_2 system cell was shown to have compelling reversibility and cycle life when SO_2 is introduced into the cell as a gas (not liquid) with $LiNTf_2$ (1 M in tetraethylene glycol dimethyl ether (TEGDME)) as the electrolyte.[124] The reversible formation/decomposition of $Li_2S_2O_4$ followed that in Reaction 8; attainable discharge voltages were slightly higher than that of Li−O_2, whereas charging voltages, which ranged from 3−4.2 V vs. Li/Li^+, were significantly lower (**Fig. 4b**). The lithium dithionite product, $Li_2S_2O_4$ (**Fig. 4a, 5**) consists of two single-electron reduction products, SO_2^-, dimerized through a central S-S bond and stabilized by two Li^+ ions. This motif in the solid phase requires breakage of only one bond upon charge to release SO_2(*g*), and thus the more-recent Li−SO_2(*g*) cell exhibits low hysteresis with appropriate choice of electrolyte, even without the use of solid catalysts. The success of this particular cell appears to lie

in use of the glyme electrolyte, which may have also supported better Li reversibility than in previous rechargeability attempts. A soluble redox mediator, LiI, was found to lower the charging voltage even further to < 3.3 V vs. Li/Li^+.[124] However, some side products (Li_2SO_3 and Li_2SO_4) were found in cycled electrodes.

Notably, unlike the $Li–O_2$ system, the reactivity of SO_2^- against organic carbonate solvents is thermodynamically and kinetically unfavorable. The same group later demonstrated that it is also feasible to utilize carbonate solvent-based electrolytes for $Li–SO_2$ cycling, which are attractive due to their large stability window particularly on charge (in contrast to ethers) and to their high conductivity, resulting in improved performance. Using another soluble redox mediator, 5,10-dimethylphenazine, the $Li–SO_2$ cell could cycle for more than 450 cycles (0.5 mAh cutoff at 1 mA/cm^2), with an overall polarization of only 0.2 V.[125] The formation of side products was somewhat mitigated, but accumulation of Li_2SO_4 could not be avoided.

Unfortunately, due to the toxicity of SO_2, widespread commercialization in EV applications is unlikely, even if better reversibility could be achieved without the use of soluble catalysts. Regardless, these interesting demonstrations-of-concept provide new insights into electrochemical and solid-phase motifs that support reversibility in gas-to-solid reactions, discussed further below.

$Li–CO_2$. Another example of oxide gas batteries is $Li–CO_2$, which has been proposed as a technology of interest for potentially extracting end-of-life value from CO_2 emissions.[126] Although a reaction forming carbon monoxide (CO) is theoretically possible on discharge,[127] the experimentally-observed reaction pathway forms only solid phases:

$$\text{Anode} : 4Li(s) \leftrightarrow 4Li^+ + 4e^-$$

$$\text{Cathode} : 3CO_2(g) + 4e^- + 4Li^+ \leftrightarrow 2Li_2CO_3(s) + C(s)$$

$$\text{Cell}: 3CO_2(g) + 4Li(s) \leftrightarrow 2Li_2CO_3(s) + C(s) \quad (9)$$

$$E^o = 2.80 \text{ V vs. } Li/Li^+, Q_{theoretical} = 670 \text{ mAh/g}, E_{theoretical} = 1880 \text{ Wh/kg}$$

Note that several elemental reaction pathways have been proposed that are consistent with this overall reaction, and are still under debate given challenges to verify the specific pathways experimentally.[128-130] Li−CO_2 electrochemistry was first studied in the context of mixed-gas Li–O_2/CO_2 batteries to investigate CO_2's role in enhancing O_2 electrochemistry[131,132] as well as its role as a possible contaminant in air-breathing O_2 cells.[133] In those systems, O_2 was shown to be the electro-active species due to more facile reduction kinetics, generating O_2^- which chemically reacts with CO_2.[132] Similar to Li-O_2 batteries, the solvent was found to play a guiding role in dictating the reaction pathway:[134] high DN solvents such as DMSO yield preferential formation of Li_2CO_3, reflecting the tendency of the solvent to support high O_2^- solubility which subsequently activates CO_2. The peroxodicarbonate anion ($C_2O_6^{2-}$) was later identified as the key intermediate in this reaction.[135] In low-DN solvents such as glymes, Li_2O_2 is the major product given the surface-localized nature of O_2 reduction and competitive disproportionation. Regardless, formation of Li_2CO_3 in these mixed-gas systems is non-reversible, releasing no O_2 on charge.[132] Later, CO_2 also became the focus of standalone gas cathode development. Archer's group reported the first primary Li–CO_2 battery based on an ionic liquid electrolyte operating at moderate temperature (60−100 °C) in 2013.[127] Subsequent efforts reported high attainable capacities in CO_2 cells at room temperature with select electrolytes. Glyme-based electrolytes are almost universally used in systems reporting high CO_2 activity and capacity with carbon electrodes; in contrast to Li−O_2 batteries, CO_2 has been observed to be largely inactive in DMSO electrolytes[132,136] albeit with some exceptions.[126] A reason for this was provided recently,[130] where it was found that the availability of Li^+ is critical to activate CO_2 reduction intermediates and facilitate completion of

the multi-electron reaction, which is favored in lower-DN solvents but precluded by higher-DN solvents. Though efforts have been made to gain insight into the complex step-wise CO_2 reduction process, the fundamental pathway is still under discussion.[131]

The Li−CO_2 system has limited reversibility. Although both C and Li_2CO_3 (**Fig. 4a**) are formed on discharge, Li_2CO_3 decomposition has received the most interest when investigating the charging process. Li_2CO_3 oxidation can occur through two reaction pathways: reaction between Li_2CO_3 and C ($2Li_2CO_3 + C \rightarrow 3CO_2 + 4Li+ + 4e^-$, E^o = 2.80 V vs. Li/Li^+), the "true" reversible battery chemistry;[137] or decomposition of Li_2CO_3 only without involving carbon, nominally forming O_2 ($2Li_2CO_3 \rightarrow 2CO_2 + O_2 + 4Li^+ + 4e^-$, E^o = 3.82 vs. Li/Li^+).[138] The second reaction is highly problematic because it can generate $^1O_2$[62] which reacts parasitically with electrolyte; $O_2(g)$ is commonly not detected upon charge.[139] In addition, due to the high thermodynamic stability of Li_2CO_3 and large bandgap (8.8 eV compared to 4.9 eV for Li_2O_2),[140] high charging overpotentials are needed (E > 4.2 V, **Fig. 4b**).[141] These high voltages exacerbate cell degradation issues including electrolyte decomposition and carbon corrosion. Thus, most efforts have focused on identifying catalysts that can promote the desired reaction pathway and address these other issues. Such efforts have been summarized previously,[138] with Mo_2C,[129] Ni,[142] Mn_2O_3,[143] and Ru[137] as some examples of catalysts that have been studied. However, charging voltages still remain too high for practical use, and the degree of electrochemical reversibility upon cycling at high depth-of-discharge (rather than capacity-limited cycling, which is often utilized) remains unclear.

It should be noted that lithium oxalate, $Li_2C_2O_4$, represents an alternative possible discharge product:

$$\text{Anode} : 2Li(s) \leftrightarrow 2Li^+ + 2e^-$$

$$\text{Cathode} : 2CO_2(g) + 2e^- + 2Li^+ \leftrightarrow Li_2C_2O_4(s)$$

$$\text{Cell}: 2CO_2(g) + 2Li(s) \leftrightarrow Li_2C_2O_4(s) \quad (10)$$

$$E^o = 3.0 \text{ V vs. } Li/Li^{+}$$ [144]

However, it has been rarely-observed in Li−CO_2 cells with few exceptions.[129] Oxalate consists of two single-electron CO_2^- radicals dimerized through the C-C bond and stabilized by two Li^+. Akin to the reversible $Li_2S_2O_4$, such a motif appears favorable for improved reversibility back to CO_2(g) compared to Li_2CO_3 + C (**Fig. 5**). However, as with Li−O_2, a dramatic shift in CO_2 electrochemical environment may be required to realize such a system.

Li−sulfur hexafluoride (Li−SF_6). The gas cathodes presented so far achieve high capacities owing to low molecular weights, though only undergo up to 2 e^-/molecule redox on discharge/charge (O_2/Li_2O_2: 2 e^-/molecule; $SO_2/Li_2S_2O_4$: 1 e^-/molecule; CO_2/Li_2CO_3: 4/3 e^-/molecule). Thus, a prospective strategy to increase specific energy further is to seek gas reactants capable of higher electron-transfer numbers. Ideally, new chemistries can also provide alternatives to strongly oxidizing gases (O_2 and SO_2), which are often undesirable to transport and store in many applications, including military and space, for safety reasons. Gallant's group demonstrated this concept with the Li−SF_6 battery in 2018. SF_6, a gas that is widely used in the microelectronics industry, contains a central sulfur atom connected octahedrally to six fluoride (F^-) ligands (**Fig. 1a**); sulfur is in its highest oxidation state (+6). It was recognized that full reduction of SF_6 can potentially accommodate up to 8 e^-/molecule by the reaction:

$$\text{Anode}: 8Li(s) \rightarrow 8Li^+ + 8e^-$$

$$\text{Cathode}: SF_6(g) + 8e^- + 8Li^+ \rightarrow 6LiF(s) + Li_2S(s)$$

$$\text{Cell}: SF_6(g) + 8Li(s) \rightarrow 6LiF(s) + Li_2S(s) \quad (11)$$

$$E^o = 3.69 \text{ V vs. } Li/Li^+, Q_{theoretical} = 1063 \text{ mAh/g}, E_{theoretical} = 3922 \text{ Wh/kg}$$

yielding a theoretical specific energy exceeding even that of Li−O_2 (**Fig. 1b,c**). Interestingly, the Li−SF_6 reaction has been used in a separate context that reflects its capability for ultrahigh-energy: as a combustion reaction underlying the Mark 50 torpedo and other naval power uses, where the thermal energy released by injection of SF_6(g) into molten Li (~540 °C) was used to power a Rankine cycle for underwater propulsion.[145] However, an electrochemical analogue was not known. As a perfluorinated gas with spherical symmetry of the ligand shell, SF_6 is widely considered chemically inert (particularly at room temperature). This makes SF_6 a safe and non-toxic reactant; on the other hand, reactions usually have high activation energies.[145]

Room-temperature reduction of SF_6 was first demonstrated in a Li−gas cell using carbon cathodes and glyme (TEGDME) electrolyte.[146] Discharge coupled to pressure measurements, along with quantitative ^{19}F NMR spectroscopy, confirmed 6 equivalents of LiF formed per SF_6 molecule reacted. Sulfur was also found in a reduced state (Li_2S) indicating that a large population of SF_6 can react fully to Li_2S, and indicating that up to 8 e^-/molecule is achievable in practice. However, the presence of some less-reduced polysulfides in the cathode and electrolyte indicated that a population of partially-reduced SF_x ($x<6$) or Li_yS_z ($y\leq2$) species are also formed and/or may react with Li_2S to yield more complex products.

The experimentally achievable discharge voltage of Li−SF_6, which was 2.2 vs Li/Li^+ in TEGDME electrolyte initially, was significantly lower than the theoretical value of 3.67 V vs. Li/Li^+, and thus accounts for the major energy loss in the cell. The voltage could be increased somewhat by changing the electrolyte to higher-DN solvents such as DMSO, reaching ~2.6 V vs Li/Li^+ and 2550 Wh/kg at the active-materials level (at 50 °C, **Fig. 1c**). The voltage change (~300 mV at room temperature, **Fig. 4c**) is consistent with the shift of the Li/Li^+ redox potential between glyme (DME) and DMSO, and may not reflect significant change in the SF_6 reduction potential.[147]

The fact that the Li^+ solvation strength may alter the attainable cell voltages indicates that Li^+ is likely not concertedly transferred in the cathode reduction reaction, but rather chemically precipitates the ejected F^- (SF_6 is known to decompose in the gas phase through anion ejection upon spark discharge activation),[148] such that it factors in the anode potential and does not cancel out in the cathode potential. The precise multi-step reduction mechanisms remain unclear as the highly complex branching over multiple electron-transfer steps evades experimental measurement to date.[149] However, the high discharge overpotential is believed to arise from sluggish activation kinetics of SF_6, which includes poor adsorption to typical carbon substrates. These kinetic limitations affect the rate capability and power of these cathodes significantly, similar to Li−O_2 systems (**Fig. 4d**). It will be of interest to determine whether catalysts, which have been shown to activate SF_6 in homogeneous contexts,[150,151] may be able to address the high overpotential issues.

Similar to Li−O_2 batteries, the electrolyte properties significantly affect solid-phase nucleation and growth of LiF, and therefore the discharge capacity. It was found that low DN solvents (such as carbonates or glyme) resulted in formation of densely-distributed LiF nucleation sites on gas diffusion electrodes at the beginning of discharge, which yielded a film-like LiF coating in the fully discharged cathode and lower attainable capacities. With high DN solvents, nucleation sites were sparser and large LiF particles were formed due to improved LiF solubility. This indicates that similar solvent-design principles are relevant with fluoride-forming reactions as with O_2^-. Adding a fluoride-binding agent (tris(pentafluorophenyl)borane) or slightly increasing the temperature (to 50 °C) were found to support increased F^- solubility and resulted in even larger LiF particles and capacities. As a result, the rate capability of the cell was significantly improved, and the attainable areal capacity was increased by ~25 times (from <0.1 to 2.3 mAh/cm^2 at 120

μA/cm^2).[152] It remains to be seen whether LiF capacities can be engineered to be comparable with that of Li−O_2 (>15 mAh/cm^2) if similar strategies are pursued with further development.

As a result of the highly irreversible S-F bond cleavage, along with high stability and electronic resistivity of the products (LiF, Li_2S) formed upon discharge, it has not been possible to re-generate these fluorinated gases by charging the cell. Note that many partial sulfur fluorides are toxic gases (such as SF_4 and S_2F_{10}), and thus attempting to re-form SF_6 should be done while exercising extreme caution. This system is thus currently considered to be a primary battery. Further developments are needed to increase the accessible discharge voltage, improve rate capability, and tap into the intrinsically high energy densities before this metal−gas battery can compete with commercial state-of-the-art including Li−$SOCl_2$ and Li−MnO_2, which benefit from higher discharge voltages (in the case of Li−$SOCl_2$, **Fig. 4c**) and higher rate capabilities than the metal−gas systems at present.

Li−nitrogen trifluoride (Li−NF_3). A second model perfluorinated gas system was also investigated by the same group. NF_3 is another low-toxicity gas that is also commonly used in microelectronics processing, and can theoretically achieve a remarkably high voltage and specific energy upon discharge:

$$\text{Anode : } 6Li(s) \rightarrow 6Li^+ + 6e^-$$

$$\text{Cathode : } 2NF_3(g) + 6e^- + 6Li^+ \rightarrow 6LiF(s) + N_2(g)$$

$$\text{Cell : } 2NF_3(g) + 6Li(s) \rightarrow 6LiF(s) + N_2(g) \qquad (12)$$

$$E^o = 5.70 \text{ V vs. } Li/Li^+,\ Q_{theoretical} = 876 \text{ mAh/g},\ E_{theoretical} = 5072 \text{ Wh/kg}$$

The high specific energy density comes mainly from the exceedingly high theoretical voltage, which reflects the high e^-/molecule transfer along with formation of highly stable N_2(*g*) and LiF as the products.[153] In practice, the attainable voltage of Li−NF_3 was found to be remarkably lower

than the theoretical, and, at ~2.3 V vs. Li/Li^+ on carbon, was even slightly lower than that of Li−SF_6 (**Fig. 4c**). The high voltage losses appear at present to be characteristic of the perfluorinated gases, although the precise reasons are not currently understood. Increasing the cell operating temperature was found to improve kinetics and thus the attainable voltage and capacity; the attainable energy could reach 1915 Wh/kg based on the weight of reactants (**Fig. 1c**), which is however still well short of the theoretical value. Like SF_6, the Li−NF_3 battery is also irreversible. Thus the ability to unlock its intrinsically high specific energy, potentially through the use of catalysts, exploration of other electrolytes, higher cell pressures or operating temperatures will be necessary to realize attractive and practical primary batteries based on this chemistry.

It should be noted that SF_6 and NF_3 are potent greenhouse gases, and thus they should be considered as model multi-electron systems at present, with possible niche applications for military and space if performance can be improved. However, the ability to realize 6-to-8 e^-/molecule reactions can hopefully spur additional research into less environmentally-problematic reactants that capitalize on the high-oxidation states accessible to S, N, C, and other non-transition metal-containing molecules beyond that of O. Along these lines, first attempts at a Li−nitrogen (N_2) battery (6 e^-/molecule, nominally forming Li_3N) have been reported, though with low cell voltages (~ 1 V vs. Li/Li^+).[154] The reported voltage is higher than the theoretical potential corresponding to formation of Li_3N (0.44 V vs. Li/Li^+), and the reduction mechanism is still being studied.

Designing new gas cathodes: chemistry and performance. As a family, Li−gas systems exhibit a wide range of performances in terms of reversibility and energy densities. Considering the future trajectory of metal−gas systems, two 'Holy Grails' can be defined, with different technology impacts: A truly rechargeable metal−gas battery with specific energy density exceeding that of Li-ion at the system level; or, on the other hand, new primary battery

formulations with energies that exceed today's state-of-the-art. While the latter does not address clean energy needs, it represents an important space for electrochemical research as primary power systems are still in widespread demand for military (ground, naval and air), space exploration, medical, and emerging robotics applications among many others where portability is crucial. Ideally, it would be possible to identify systems that can achieve both ultrahigh energy and reversibility. Thus, it is worth investigating whether such systems are possible or, instead, face fundamental physiochemical and electrochemical limits.

One factor relating to reversibility of gas reactants is the hardness of the reactant-state molecule, which determines to what extent reduction is favored as well as the ensuing electronic reconfiguration as the gas reacts to the solid phase. The definition of absolute hardness (η) given by Parr and Pearson is:[155]

$$\eta = \frac{1}{2}\left(\frac{\partial^2 E}{\partial N^2}\right) \sim \frac{I - A}{2}$$

where E is the energy, N is the total number of electrons, I is the ionization potential and A is the electron affinity (EA). I is related to the energy level of the highest occupied molecular orbital (HOMO) or the singly occupied molecular orbital (SOMO), such that $I = -\varepsilon_{\mathrm{HOMO(SOMO)}}$. For molecules with a fully-filled HOMO, the electron affinity is related to the energy of the lowest unoccupied molecular orbital (LUMO): $A = -\varepsilon_{\mathrm{LUMO}}$, thus the hardness is the energy difference between HOMO and LUMO. The larger the HOMO/LUMO gap ($\sim 2\eta$), the higher the molecule hardness η. In contrast, for molecules with unpaired electrons, the hardness is determined by the electron repulsion energy in the SOMO (the LUMO energy becomes irrelevant).[156]

Based on the hard-soft (Lewis) acid-base (HSAB) theory, electron-transfer events favor soft/soft interactions[157] in which the electronic structure of the molecule can gently re-configure to accommodate the added charge into available molecular orbitals without drastic restructuring,

the latter of which includes reduction of bond orders down to 0. This indicates that soft gas molecules will be more likely to support a reversible electron transfer. As is shown in **Fig. 5a**, except for O_2 which has unpaired electrons, the HOMO of the remaining molecules are all filled, such that the first electron enters above a significant HOMO/LUMO gap. Among these, SO_2 exhibits the smallest HOMO/LUMO gap of 5.37 eV, and is thus softest. As for O_2, the EA is ~0.45 eV,[158] resulting in $2\eta \approx 7.93$ eV, which is the second-lowest among the five molecules.[159] O_2 can also accommodate two electrons in the π^* orbitals; the bond order reduces by 1 but is not fully broken. This reasoning agrees with experimental observations in which SO_2 and O_2 exhibit facile discharge behavior compared to the theoretical voltages (**Fig. 1c**) and relatively minor structural reconfiguration upon incorporation into the solid phase—O-O bonds or S-O bonds are still retained (**Fig. 5b**). In contrast, the three "hard" molecules, CO_2, SF_6, and NF_3, are less favored for electron transfer: Li−CO_2 batteries exhibit relatively limited rate performance and catalysts are usually needed, while Li−SF_6 and Li−NF_3 batteries still burdened by large discharge overpotentials which can be attributed to sluggish kinetics of the first electron transfer. In addition, for SF_6 and NF_3, all S-F or N-F bonds are broken during reduction to accommodate the large number of electrons per molecule. The extensive bond-breaking process makes it nearly impossible to reconstruct the gas molecules from the highly stable products (Li_2S, LiF, or N_2). Similar is true for Li−CO_2 batteries; though the detailed reaction mechanism remains unclear, the formation of C indicates some extent of C-O bond breaking; meanwhile the formation of the highly stable Li_2CO_3 makes recharge highly challenging. Overall, there is an apparent trade-off between specific energy and the reversibility: multiple bond-breaking enables multi-electron transfer reactions and is facilitated by high stability of the formed products; however, this simultaneously increases the complexity for the backward reaction. It remains to be seen whether a compromise can be reached in terms of electron transfers

>2 while retaining mass-efficiency (light weight of the gas), forming only moderately stable solid phases (less stable than LiF, Li_2CO_3, and even Li_2O_2) that are more amenable to recharge, and gaining improved control over electrochemical pathway to avoid parasitic chemistry of gas radicals and unlock long cycle life. In spite of this tall order, numerous platforms for a next generation of primary batteries have already been identified as reviewed herein. These platforms promise to continue to deepen the community's fundamental understanding of molecular electrochemistry, while practically re-invigorating the historically important and successful area of metal−gas technology development.

Perspective

The rechargeable metal−O_2 battery family saw an initial enthusiasm for attainable performance based on exceptional theoretical metrics in the Li−O_2 system, which has yet to be realized as a truly reversible cell. Subsequent strategies to address the Achilles' heel of Li−O_2 – chemical reactivity and poor reversibility – saw a rich exploration of new concepts related to oxygen cathode electrochemistry and an expansion of the types of metal anodes under serious consideration for rechargeable batteries, however each with tradeoffs. None has matched the Li−O_2 battery's initial promise in terms of performance metrics, nor have the reactivity issues involving reactive oxygen redox in organic media been solved. Meanwhile, rechargeability has been achieved with a scaling-back of energy expectations, while introducing new, challenging issues of cathode and anode side-reactions.

Given severe reversibility issues, development so far has tended to focus on characterization of batteries at low rates where promising performance, along with intrinsic reactivity issues, can be best identified. For EV applications, the power of metal−gas batteries remains too low. Meanwhile, the chemical reactivity issues have precluded much focus on long-

term cycling, with many papers reporting tens of cycles or fewer, whereas Li-ion batteries can cycle up to thousands of cycles. If truly reversible chemistry and electrochemistry can be identified, the field is arguably primed to undertake rapid engineering development of metal−O_2 batteries given the significant expertise built over the last decade.

Remarkable scientific progress has been made in understanding the electrochemistry of gas-based conversion reactions in nonaqueous environments. This includes the critical role played by the electrolyte, which was found to no longer be a passive bystander for sustaining ionic current as with Li-ion batteries, but rather a central player in the reaction pathway. In addition, the limits of molecular oxygen redox have been arguably pushed farther than ever before as researchers considered new bonding environments and sources of 'O' and learned how these factors affect reactivity and reversibility. These efforts laid the groundwork for future chemistry development, which may include identification of new reactants entirely or opportunities for more complex redox engineering, including concepts such as mixed-gas and hybrid liquid-gas cathodes.

Along the way, expectations shifted for possible applications. Regardless of the future of O_2 as a reversible gas cathode, new and compelling motifs for improved primary batteries were identified, with a host of engineering strategies (electrolyte, redox mediators, cathode and anode design) now available to design improved performance. As shown herein, such batteries need not operate on O_2; in many applications where safety is critical and carrying an on-board oxidant may be undesirable, fluorinated gases may provide a possible path forward. Ultimately, it will be important to learn from these new chemistries and their unique redox mechanisms to continue to identify novel reactants capable of high voltages and high power. Building on the success of "liquid O" reactants, as demonstrated for the molten nitrate systems, it will be intriguing to investigate whether other liquid oxygen-bearing and/or fluorinated analogues exist which can start to move

the dial of these primary batteries into strongly competitive territory with today's commercialized systems.

References

1 Office of Energy Efficiency and Renewable Energy, US DRIVE electrochemical energy storage roadmap (2017). https://www.energy.gov/eere/vehicles/downloads/us-drive-electrochemical-energy-storage-technical-team-roadmap. Accessed 21 May 2020.

2 Schmuch, R., Wagner, R., Hörpel, G., Placke, T. & Winter, M. Performance and cost of materials for lithium-based rechargeable automotive batteries. *Nat. Energy* **3**, 267-278 (2018).

3 Whittingham, M. S. Ultimate limits to intercalation reactions for lithium batteries. *Chem. Rev.* **114**, 11414-11443 (2014).

4 Nitta, N., Wu, F., Lee, J. T. & Yushin, G. Li-ion battery materials: present and future. *Mater. Today* **18**, 252-264 (2015).

5 Wu, F. & Yushin, G. Conversion cathodes for rechargeable lithium and lithium-ion batteries. *Energy Environ. Sci.* **10**, 435-459 (2017).

6 Cabana, J., Monconduit, L., Larcher, D. & Palacin, M. R. Beyond intercalation‐based Li‐ion batteries: the state of the art and challenges of electrode materials reacting through conversion reactions. *Adv. Mater.* **22**, E170-E192 (2010).

7 Bruce, P. G., Freunberger, S. A., Hardwick, L. J. & Tarascon, J.-M. Li–O_2 and Li–S batteries with high energy storage. *Nat. Mater.* **11**, 19-29 (2012).

8 Pang, Q., Liang, X., Kwok, C. Y. & Nazar, L. Advances in lithium–sulfur batteries based on multifunctional cathodes and electrolytes. *Nat. Energy* **1**, 1-11 (2016).

9 Manthiram, A., Chung, S. H. & Zu, C. Lithium–sulfur batteries: progress and prospects. *Adv. Mater.* **27**, 1980-2006 (2015).

10 Blurton, K. F. & Sammells, A. F. Metal/air batteries: their status and potential—a review. *J. Power Sources* **4**, 263-279 (1979).

11 Meyers, W. F. & Simmons, J. W. Electric current-producing cell with anhydrous organic liquid electrolyte. U.S. patent (1969).

12 Abraham, K. & Jiang, Z. A polymer electrolyte‐based rechargeable lithium/oxygen battery. *J. Electrochem. Soc.* **143**, 1-5 (1996).

13 Ogasawara, T., Débart, A., Holzapfel, M., Novák, P. & Bruce, P. G. Rechargeable Li_2O_2 electrode for lithium batteries. *J. Am. Chem. Soc.* **128**, 1390-1393 (2006).

14 Débart, A., Paterson, A. J., Bao, J. & Bruce, P. G. α‐MnO_2 nanowires: A catalyst for the O_2 electrode in rechargeable lithium batteries. *Angew. Chem., Int. Ed.* **47**, 4521-4524 (2008).

15 Lu, Y.-C. *et al.* Platinum−gold nanoparticles: a highly active bifunctional electrocatalyst for rechargeable lithium−air batteries. *J. Am. Chem. Soc.* **132**, 12170-12171 (2010).

16 Kwak, W.-J. *et al.* Lithium–oxygen batteries and related systems: potential, status, and future. *Chem. Rev.* (2020).

17 Liu, T. *et al.* Current challenges and routes forward for nonaqueous lithium–air batteries. *Chem. Rev.* (2020).

18 Lu, Y.-C. *et al.* Lithium–oxygen batteries: bridging mechanistic understanding and battery performance. *Energy Environ. Sci.* **6**, 750-768 (2013).

19 Read, J. *et al.* Oxygen transport properties of organic electrolytes and performance of lithium/oxygen battery. *J. Electrochem. Soc.* **150**, A1351 (2003).
20 Lu, Y.-C. *et al.* The discharge rate capability of rechargeable Li–O_2 batteries. *Energy Environ. Sci.* **4**, 2999-3007 (2011).
21 Johnson, L. *et al.* The role of LiO_2 solubility in O_2 reduction in aprotic solvents and its consequences for Li–O_2 batteries. *Nat. Chem.* **6**, 1091 (2014).
22 Mitchell, R. R., Gallant, B. M., Shao-Horn, Y. & Thompson, C. V. Mechanisms of morphological evolution of Li_2O_2 particles during electrochemical growth. *J. Phys. Chem. Lett.* **4**, 1060-1064 (2013).
23 Lau, S. & Archer, L. A. Nucleation and growth of lithium peroxide in the Li–O2 battery. *Nano Lett.* **15**, 5995-6002 (2015).
24 Gallant, B. M. *et al.* in *The Lithium Air Battery: Fundamentals* (eds Nobuyuki Imanishi, Alan C. Luntz, & Peter Bruce) Ch. 4, 121-158 (Springer New York, 2014).
25 Rabenau, A. Lithium nitride and related materials case study of the use of modern solid state research techniques. *Solid State Ionics* **6**, 277-293 (1982).
26 Girishkumar, G., McCloskey, B., Luntz, A. C., Swanson, S. & Wilcke, W. Lithium−air battery: promise and challenges. *J. Phys. Chem. Lett.* **1**, 2193-2203 (2010).
27 Meini, S., Piana, M., Tsiouvaras, N., Garsuch, A. & Gasteiger, H. A. The effect of water on the discharge capacity of a non-catalyzed carbon cathode for Li-O_2 batteries. *Electrochem. Solid-State Lett.* **15**, A45 (2012).
28 Gallagher, K. G. *et al.* Quantifying the promise of lithium–air batteries for electric vehicles. *Energy Environ. Sci.* **7**, 1555-1563 (2014).
29 Freunberger, S. A. *et al.* Reactions in the rechargeable lithium–O_2 battery with alkyl carbonate electrolytes. *J. Am. Chem. Soc.* **133**, 8040-8047 (2011).
30 McCloskey, B. D., Bethune, D. S., Shelby, R. M., Girishkumar, G. & Luntz, A. C. Solvents' critical role in nonaqueous lithium–oxygen battery electrochemistry. *J. Phys. Chem. Lett.* **2**, 1161-1166 (2011).
31 McCloskey, B. D. *et al.* On the efficacy of electrocatalysis in nonaqueous Li–O_2 batteries. *J. Am. Chem. Soc.* **133**, 18038-18041 (2011).
32 Aurbach, D., McCloskey, B. D., Nazar, L. F. & Bruce, P. G. Advances in understanding mechanisms underpinning lithium–air batteries. *Nat. Energy* **1**, 16128 (2016).
33 Peng, Z. *et al.* Oxygen reactions in a non‐aqueous Li^+ electrolyte. *Angew. Chem., Int. Ed.* **50**, 6351-6355 (2011).
34 Yu, Q. & Ye, S. In situ study of oxygen reduction in dimethyl sulfoxide (DMSO) solution: a fundamental study for development of the lithium–oxygen battery. *J. Phys. Chem. C* **119**, 12236-12250 (2015).
35 Galloway, T. A. & Hardwick, L. J. Utilizing in situ electrochemical SHINERS for oxygen reduction reaction studies in aprotic electrolytes. *J. Phys. Chem. Lett.* **7**, 2119-2124 (2016).
36 Viswanathan, V. *et al.* Electrical conductivity in Li_2O_2 and its role in determining capacity limitations in non-aqueous Li-O_2 batteries. *J. Chem. Phys.* **135**, 214704 (2011).
37 Gallant, B. M. *et al.* Influence of Li_2O_2 morphology on oxygen reduction and evolution kinetics in Li–O_2 batteries. *Energy Environ. Sci.* **6**, 2518-2528 (2013).
38 Laoire, C. O., Mukerjee, S., Abraham, K., Plichta, E. J. & Hendrickson, M. A. Influence of nonaqueous solvents on the electrochemistry of oxygen in the rechargeable lithium− air battery. *J. Phys. Chem. C* **114**, 9178-9186 (2010).

39 Burke, C. M., Pande, V., Khetan, A., Viswanathan, V. & McCloskey, B. D. Enhancing electrochemical intermediate solvation through electrolyte anion selection to increase nonaqueous Li–O_2 battery capacity. *Proc. Natl. Acad. Sci.* **112**, 9293-9298 (2015).

40 Aetukuri, N. B. *et al.* Solvating additives drive solution-mediated electrochemistry and enhance toroid growth in non-aqueous Li–O_2 batteries. *Nat. Chem.* **7**, 50 (2015).

41 Schwenke, K. U., Metzger, M., Restle, T., Piana, M. & Gasteiger, H. A. The influence of water and protons on Li_2O_2 crystal growth in aprotic Li-O_2 cells. *J. Electrochem. Soc.* **162**, A573-A584 (2015).

42 Gao, X., Chen, Y., Johnson, L. & Bruce, P. G. Promoting solution phase discharge in Li–O_2 batteries containing weakly solvating electrolyte solutions. *Nat. Mater.* **15**, 882 (2016).

43 Lee, D. *et al.* Direct observation of redox mediator-assisted solution-phase discharging of Li–O_2 battery by liquid-phase transmission electron microscopy. *J. Am. Chem. Soc.* **141**, 8047-8052 (2019).

44 Liu, T. *et al.* The effect of water on quinone redox mediators in nonaqueous Li-O_2 batteries. *J. Am. Chem. Soc.* **140**, 1428-1437 (2018).

45 Peng, Z., Chen, Y., Bruce, P. G. & Xu, Y. Direct detection of the superoxide anion as a stable intermediate in the electroreduction of oxygen in a non‐aqueous electrolyte containing phenol as a proton source. *Angew. Chem., Int. Ed.* **54**, 8165-8168 (2015).

46 Gao, X., Jovanov, Z. P., Chen, Y., Johnson, L. R. & Bruce, P. G. Phenol‐catalyzed discharge in the aprotic lithium‐oxygen battery. *Angew. Chem.* **129**, 6639-6643 (2017).

47 Ko, Y. *et al.* Biological redox mediation in electron transport chain of bacteria for oxygen reduction reaction catalysts in lithium–oxygen batteries. *Adv. Funct. Mater.* **29**, 1805623 (2019).

48 Zhang, Y. *et al.* High‐capacity and high‐rate discharging of a coenzyme Q_{10}‐catalyzed Li‐O_2 battery. *Adv. Mater.* **30**, 1705571 (2018).

49 Park, J. B., Lee, S. H., Jung, H. G., Aurbach, D. & Sun, Y. K. Redox mediators for Li–O_2 batteries: status and perspectives. *Adv. Mater.* **30**, 1704162 (2018).

50 Liang, Z., Zhou, Y. & Lu, Y.-C. Dynamic oxygen shield eliminates cathode degradation in lithium–oxygen batteries. *Energy Environ. Sci.* **11**, 3500-3510 (2018).

51 Lu, J. *et al.* Aprotic and aqueous Li–O_2 batteries. *Chem. Rev.* **114**, 5611-5640 (2014).

52 Chang, Z., Xu, J. & Zhang, X. Recent progress in electrocatalyst for Li‐O_2 batteries. *Adv. Energy Mater.* **7**, 1700875 (2017).

53 Ko, Y., Park, H., Kim, B., Kim, J. S. & Kang, K. Redox mediators: a solution for advanced lithium–oxygen batteries. *Trends Chem.* **1**, 349-360 (2019).

54 Khetan, A., Luntz, A. & Viswanathan, V. Trade-offs in capacity and rechargeability in nonaqueous Li–O_2 batteries: solution-driven growth versus nucleophilic stability. *J. Phys. Chem. Lett.* **6**, 1254-1259 (2015).

55 Wang, Y. *et al.* A solvent-controlled oxidation mechanism of Li_2O_2 in lithium-oxygen batteries. *Joule* **2**, 2364-2380 (2018).

56 Ottakam Thotiyl, M. M., Freunberger, S. A., Peng, Z. & Bruce, P. G. The carbon electrode in nonaqueous Li–O_2 cells. *J. Am. Chem. Soc.* **135**, 494-500 (2012).

57 Black, R. *et al.* Screening for superoxide reactivity in Li-O_2 batteries: effect on Li_2O_2/LiOH crystallization. *J. Am. Chem. Soc.* **134**, 2902-2905 (2012).

58 Zhang, X. *et al.* LiO_2: cryosynthesis and chemical/electrochemical reactivities. *J. Phys. Chem. Lett.* **8**, 2334-2338 (2017).

59 Wandt, J., Jakes, P., Granwehr, J., Gasteiger, H. A. & Eichel, R. A. Singlet oxygen formation during the charging process of an aprotic lithium–oxygen battery. *Angew. Chem., Int. Ed.* **55**, 6892-6895 (2016).
60 Mahne, N. *et al.* Singlet oxygen generation as a major cause for parasitic reactions during cycling of aprotic lithium–oxygen batteries. *Nat. Energy* **2**, 1-9 (2017).
61 Mourad, E. *et al.* Singlet oxygen from cation driven superoxide disproportionation and consequences for aprotic metal–O_2 batteries. *Energy Environ. Sci.* **12**, 2559-2568 (2019).
62 Mahne, N., Renfrew, S. E., McCloskey, B. D. & Freunberger, S. A. Electrochemical oxidation of lithium carbonate generates singlet oxygen. *Angew. Chem., Int. Ed.* **57**, 5529-5533 (2018).
63 Freunberger, S. A. *et al.* The lithium – oxygen battery with ether - based electrolytes. *Angew. Chem., Int. Ed.* **50**, 8609-8613 (2011).
64 Sharon, D. *et al.* Oxidation of dimethyl sulfoxide solutions by electrochemical reduction of oxygen. *J. Phys. Chem. Lett.* **4**, 3115-3119 (2013).
65 McCloskey, B. D. *et al.* Twin problems of interfacial carbonate formation in nonaqueous Li–O_2 batteries. *J. Phys. Chem. Lett.* **3**, 997-1001 (2012).
66 Lu, Y.-C. & Shao-Horn, Y. Probing the reaction kinetics of the charge reactions of nonaqueous Li–O_2 batteries. *J. Phys. Chem. Lett.* **4**, 93-99 (2013).
67 Peng, Z., Freunberger, S. A., Chen, Y. & Bruce, P. G. A reversible and higher-rate Li-O_2 battery. *Science* **337**, 563-566 (2012).
68 Thotiyl, M. M. O. *et al.* A stable cathode for the aprotic Li–O_2 battery. *Nat. Mater.* **12**, 1050 (2013).
69 Adams, B. D. *et al.* The importance of nanometric passivating films on cathodes for Li–air batteries. *ACS Nano* **8**, 12483-12493 (2014).
70 Kundu, D., Black, R., Berg, E. J. & Nazar, L. F. A highly active nanostructured metallic oxide cathode for aprotic Li–O_2 batteries. *Energy Environ. Sci.* **8**, 1292-1298 (2015).
71 Chen, Y., Freunberger, S. A., Peng, Z., Fontaine, O. & Bruce, P. G. Charging a Li–O_2 battery using a redox mediator. *Nat. Chem.* **5**, 489 (2013).
72 Lim, H.-D. *et al.* Rational design of redox mediators for advanced Li–O_2 batteries. *Nat. Energy* **1**, 16066 (2016).
73 Chen, Y., Gao, X., Johnson, L. R. & Bruce, P. G. Kinetics of lithium peroxide oxidation by redox mediators and consequences for the lithium–oxygen cell. *Nat. Commun.* **9**, 767 (2018).
74 McCloskey, B. D. & Addison, D. A viewpoint on heterogeneous electrocatalysis and redox mediation in nonaqueous Li-O_2 batteries. *ACS Catal.* **7**, 772–778 (2017).
75 Wang, Y., Liang, Z., Zou, Q., Cong, G. & Lu, Y.-C. Mechanistic insights into catalyst-assisted nonaqueous oxygen evolution reaction in lithium–oxygen batteries. *J. Phys. Chem. C* **120**, 6459-6466 (2016).
76 Liang, Z. & Lu, Y.-C. Critical role of redox mediator in suppressing charging instabilities of lithium–oxygen batteries. *J. Am. Chem. Soc.* **138**, 7574-7583 (2016).
77 Lim, H. D. *et al.* Superior rechargeability and efficiency of lithium–oxygen batteries: hierarchical air electrode architecture combined with a soluble catalyst. *Angew. Chem., Int. Ed.* **53**, 3926-3931 (2014).
78 Liu, T. *et al.* Cycling Li-O_2 batteries via LiOH formation and decomposition. *Science* **350**, 530-533 (2015).
79 Tułodziecki, M. *et al.* The role of iodide in the formation of lithium hydroxide in lithium–oxygen batteries. *Energy Environ. Sci.* **10**, 1828-1842 (2017).

80 Kwak, W.-J. *et al.* Deactivation of redox mediators in lithium-oxygen batteries by singlet oxygen. *Nat. Commun.* **10**, 1-8 (2019).
81 Tikekar, M. D., Choudhury, S., Tu, Z. & Archer, L. A. Design principles for electrolytes and interfaces for stable lithium-metal batteries. *Nat. Energy* **1**, 1-7 (2016).
82 Assary, R. S. *et al.* The effect of oxygen crossover on the anode of a Li–O_2 battery using an ether‐based solvent: insights from experimental and computational studies. *ChemSusChem* **6**, 51-55 (2013).
83 Lopez, N. *et al.* Reversible reduction of oxygen to peroxide facilitated by molecular recognition. *Science* **335**, 450-453 (2012).
84 Lu, J. *et al.* A lithium–oxygen battery based on lithium superoxide. *Nature* **529**, 377 (2016).
85 Kwak, W.-J., Park, J.-B., Jung, H.-G. & Sun, Y.-K. Controversial topics on lithium superoxide in Li–O_2 batteries. *ACS Energy Lett.* **2**, 2756-2760 (2017).
86 Papp, J. K. *et al.* Poly (vinylidene fluoride)(PVDF) binder degradation in Li–O_2 batteries: a consideration for the characterization of lithium superoxide. *J. Phys. Chem. Lett.* **8**, 1169-1174 (2017).
87 Giordani, V. *et al.* A molten salt lithium–oxygen battery. *J. Am. Chem. Soc.* **138**, 2656-2663 (2016).
88 Xia, C., Kwok, C. & Nazar, L. F. A high-energy-density lithium-oxygen battery based on a reversible four-electron conversion to lithium oxide. *Science* **361**, 777-781 (2018).
89 Giordani, V. *et al.* Rechargeable-battery chemistry based on lithium oxide growth through nitrate anion redox. *Nat. Chem.* **11**, 1133-1138 (2019).
90 Grimaud, A., Hong, W. T., Shao-Horn, Y. & Tarascon, J.-M. Anionic redox processes for electrochemical devices. *Nat. Mater.* **15**, 121-126 (2016).
91 Assat, G. & Tarascon, J.-M. Fundamental understanding and practical challenges of anionic redox activity in Li-ion batteries. *Nat. Energy* **3**, 373-386 (2018).
92 Zhu, Z. *et al.* Anion-redox nanolithia cathodes for Li-ion batteries. *Nat. Energy* **1**, 16111 (2016).
93 Qiao, Y., Jiang, K., Deng, H. & Zhou, H. A high-energy-density and long-life lithium-ion battery via reversible oxide–peroxide conversion. *Nat. Catal.* **2**, 1035-1044 (2019).
94 Hartmann, P. *et al.* A rechargeable room-temperature sodium superoxide (NaO_2) battery. *Nat. Mater.* **12**, 228 (2013).
95 Hartmann, P. *et al.* Discharge and charge reaction paths in sodium–oxygen batteries: Does NaO_2 form by direct electrochemical growth or by precipitation from solution? *J. Phys. Chem. C* **119**, 22778-22786 (2015).
96 Xia, C., Black, R., Fernandes, R., Adams, B. & Nazar, L. F. The critical role of phase-transfer catalysis in aprotic sodium oxygen batteries. *Nat. Chem.* **7**, 496 (2015).
97 Xia, C. *et al.* Direct evidence of solution-mediated superoxide transport and organic radical formation in sodium-oxygen batteries. *J. Am. Chem. Soc.* **138**, 11219-11226 (2016).
98 McCloskey, B. D., Garcia, J. M. & Luntz, A. C. Chemical and electrochemical differences in nonaqueous Li–O_2 and Na–O_2 batteries. *J. Phys. Chem. Lett.* **5**, 1230-1235 (2014).
99 Bender, C. L., Schröder, D., Pinedo, R., Adelhelm, P. & Janek, J. One‐ or two‐electron transfer? The ambiguous nature of the discharge products in sodium–oxygen batteries. *Angew. Chem., Int. Ed.* **55**, 4640-4649 (2016).
100 Ortiz-Vitoriano, N. *et al.* Rate-dependent nucleation and growth of NaO_2 in Na–O_2 batteries. *J. Phys. Chem. Lett.* **6**, 2636-2643 (2015).

101 Bender, C. L., Hartmann, P., Vračar, M., Adelhelm, P. & Janek, J. On the thermodynamics, the role of the carbon cathode, and the cycle life of the sodium superoxide (NaO_2) battery. *Adv. Energy Mater.* **4**, 1301863 (2014).
102 Kim, J. *et al.* Dissolution and ionization of sodium superoxide in sodium–oxygen batteries. *Nat. Commun.* **7**, 1-9 (2016).
103 Sayed, S. Y. *et al.* Revealing instability and irreversibility in nonaqueous sodium–O_2 battery chemistry. *Chem. Commun.* **52**, 9691-9694 (2016).
104 Landa-Medrano, I. *et al.* Sodium–oxygen battery: steps toward reality. *J. Phys. Chem. Lett.* **7**, 1161-1166 (2016).
105 Adelhelm, P. *et al.* From lithium to sodium: cell chemistry of room temperature sodium–air and sodium–sulfur batteries. *Beilstein J. Nanotechnol.* **6**, 1016-1055 (2015).
106 Nichols, J. E. & McCloskey, B. D. The sudden death phenomena in nonaqueous Na–O2 batteries. *J. Phys. Chem. C* **121**, 85-96 (2017).
107 Black, R. *et al.* The nature and impact of side reactions in glyme ‐ based sodium ‐ oxygen batteries. *ChemSusChem* **9**, 1795-1803 (2016).
108 Lutz, L. *et al.* Role of electrolyte anions in the Na–O_2 battery: implications for NaO_2 solvation and the stability of the sodium solid electrolyte interphase in glyme ethers. *Chem. Mater.* **29**, 6066-6075 (2017).
109 Ren, X. & Wu, Y. A low-overpotential potassium–oxygen battery based on potassium superoxide. *J. Am. Chem. Soc.* **135**, 2923-2926 (2013).
110 Qin, L., Schkeryantz, L., Zheng, J., Xiao, N. & Wu, Y. Superoxide-based K–O_2 batteries: highly reversible oxygen redox solves challenges in air electrodes. *J. Am. Chem. Soc.* (2020).
111 Wang, W., Lai, N. C., Liang, Z., Wang, Y. & Lu, Y. C. Superoxide stabilization and a universal KO_2 growth mechanism in potassium–oxygen batteries. *Angew. Chem., Int. Ed.* **57**, 5042-5046 (2018).
112 Xiao, N., Rooney, R. T., Gewirth, A. A. & Wu, Y. The Long ‐ Term Stability of KO_2 in K ‐ O_2 Batteries. *Angew. Chem., Int. Ed.* **57**, 1227 ‐ 1231 (2018).
113 Xiao, N., Gourdin, G. & Wu, Y. Simultaneous stabilization of potassium metal and superoxide in K–O_2 batteries on the basis of electrolyte reactivity. *Angew. Chem., Int. Ed.* **57**, 10864-10867 (2018).
114 Ren, X., He, M., Xiao, N., McCulloch, W. D. & Wu, Y. Greatly enhanced anode stability in K ‐ oxygen batteries with an in situ formed solvent ‐ and oxygen ‐ impermeable protection layer. *Adv. Energy Mater.* **7** (2017).
115 Qin, L., Xiao, N., Zhang, S., Chen, X. & Wu, Y. From K ‐ O_2 to K ‐ air batteries: realizing superoxide batteries on the basis of dry ambient air. *Angew. Chem.* (2020).
116 Cong, G., Wang, W., Lai, N.-C., Liang, Z. & Lu, Y.-C. A high-rate and long-life organic–oxygen battery. *Nat. Mater.* **18**, 390 (2019).
117 Li, C. S., Sun, Y., Gebert, F. & Chou, S. L. Current progress on rechargeable magnesium–air battery. *Adv. Energy Mater.* **7**, 1700869 (2017).
118 Reinsberg, P., Bondue, C. J. & Baltruschat, H. Calcium–oxygen batteries as a promising alternative to sodium–oxygen batteries. *J. Phys. Chem. C* **120**, 22179-22185 (2016).
119 Reddy, T. B. *Linden's handbook of batteries*. Vol. 4 (McGraw-Hill 2011).
120 Xing, H. *et al.* Ambient lithium–SO_2 batteries with ionic liquids as electrolytes. *Angew. Chem., Int. Ed.* **53**, 2099-2103 (2014).
121 Maricle, D. L. & Mohns, J. P. Electrochemical cell containing sulfur dioxide as the cathode depolarizer. (1971).

122 Dey, A., Kuo, H., Piliero, P. & Kallianidis, M. Inorganic electrolyte Li/SO_2 rechargeable system: development of a prototype hermetic C cell and evaluation of its performance and safety characteristics. *J. Electrochem. Soc.* **135**, 2115 (1988).
123 Fey, G.-K. Li/SO_2 rechargeable batteries. *J. Power Sources* **35**, 153-162 (1991).
124 Lim, H. D. *et al.* A new perspective on Li–SO_2 batteries for rechargeable systems. *Angew. Chem., Int. Ed.* **54**, 9663-9667 (2015).
125 Park, H. *et al.* High-efficiency and high-power rechargeable lithium–sulfur dioxide batteries exploiting conventional carbonate-based electrolytes. *Nat. Commun.* **8**, 14989 (2017).
126 Qiao, Y. *et al.* Li-CO_2 electrochemistry: a new strategy for CO_2 fixation and energy storage. *Joule* **1**, 359-370 (2017).
127 Xu, S., Das, S. K. & Archer, L. A. The Li–CO_2 battery: A novel method for CO_2 capture and utilization. *RSC Adv.* **3**, 6656-6660 (2013).
128 Xie, J. & Wang, Y. Recent Development of CO_2 Electrochemistry from Li−CO_2 Batteries to Zn−CO_2 Batteries. *Acc. Chem. Res.* (2019).
129 Hou, Y. *et al.* Mo_2C/CNT: an efficient catalyst for rechargeable Li–CO_2 batteries. *Adv. Funct. Mater.* **27**, 1700564 (2017).
130 Khurram, A., Yin, Y., Yan, L., Zhao, L. & Gallant, B. M. Governing role of solvent on discharge activity in lithium–CO_2 batteries. *J. Phys. Chem. Lett.* **10**, 6679-6687 (2019).
131 Takechi, K., Shiga, T. & Asaoka, T. A Li–O_2/CO_2 battery. *Chem. Commun.* **47**, 3463-3465 (2011).
132 Yin, W., Grimaud, A., Lepoivre, F., Yang, C. & Tarascon, J. M. Chemical vs electrochemical formation of Li_2CO_3 as a discharge product in Li–O_2/CO_2 batteries by controlling the superoxide intermediate. *J. Phys. Chem. Lett.* **8**, 214-222 (2017).
133 Gowda, S. R., Brunet, A., Wallraff, G. & McCloskey, B. D. Implications of CO2 contamination in rechargeable nonaqueous Li–O_2 batteries. *J. Phys. Chem. Lett.* **4**, 276-279 (2013).
134 Lim, H.-K. *et al.* Toward a lithium–"air" battery: the effect of CO_2 on the chemistry of a lithium–oxygen cell. *J. Am. Chem. Soc.* **135**, 9733-9742 (2013).
135 Zhao, Z., Su, Y. & Peng, Z. Probing lithium carbonate formation in Trace-O_2-assisted aprotic Li-CO_2 batteries using in situ surface-enhanced raman spectroscopy. *J. Phys. Chem. Lett.* **10**, 322-328 (2019).
136 Khurram, A., He, M. & Gallant, B. M. Tailoring the discharge reaction in Li-CO_2 batteries through incorporation of CO_2 capture chemistry. *Joule* **2**, 2649-2666 (2018).
137 Yang, S. *et al.* A reversible lithium–CO_2 battery with Ru nanoparticles as a cathode catalyst. *Energy Environ. Sci.* **10**, 972-978 (2017).
138 Liu, B. *et al.* Recent advances in understanding Li–CO_2 electrochemistry. *Energy Environ. Sci.* **12**, 887-922 (2019).
139 Yang, S., He, P. & Zhou, H. Exploring the electrochemical reaction mechanism of carbonate oxidation in Li–air/CO_2 battery through tracing missing oxygen. *Energy Environ. Sci.* **9**, 1650-1654 (2016).
140 Garcia-Lastra, J. M., Myrdal, J. S., Christensen, R., Thygesen, K. S. & Vegge, T. DFT+ U study of polaronic conduction in Li_2O_2 and Li_2CO_3: implications for Li–Air batteries. *J. Phys. Chem. C* **117**, 5568-5577 (2013).
141 Ling, C., Zhang, R., Takechi, K. & Mizuno, F. Intrinsic barrier to electrochemically decompose Li_2CO_3 and LiOH. *J. Phys. Chem. C* **118**, 26591-26598 (2014).

142 Zhang, Z. *et al.* Verifying the rechargeability of Li‐CO_2 batteries on working cathodes of Ni nanoparticles highly dispersed on N‐doped graphene. *Adv. Sci.* **5**, 1700567 (2018).
143 Ma, W., Lu, S., Lei, X., Liu, X. & Ding, Y. J. J. o. M. C. A. Porous Mn_2O_3 cathode for highly durable Li–CO_2 batteries. *J. Mater. Chem. A* **6**, 20829-20835 (2018).
144 Németh, K. & Srajer, G. CO_2/oxalate cathodes as safe and efficient alternatives in high energy density metal–air type rechargeable batteries. *RSC Adv.* **4**, 1879-1885 (2014).
145 Hughes, T., Smith, R. & Kiely, D. Stored chemical energy propulsion system for underwater applications. *J. Energy* **7**, 128-133 (1983).
146 Li, Y., Khurram, A. & Gallant, B. M. A high-capacity lithium–gas battery based on sulfur fluoride conversion. *J. Phys. Chem. C* **122**, 7128-7138 (2018).
147 Kwabi, D. G. *et al.* Experimental and computational analysis of the solvent‐dependent O_2/Li^+‐O^{2-} redox couple: standard potentials, coupling strength, and implications for lithium–oxygen Batteries. *Angew. Chem., Int. Ed.* **55**, 3129-3134 (2016).
148 Zámostná, L. & Braun, T. Catalytic degradation of sulfur hexafluoride by rhodium complexes. *Angew. Chem.* **127**, 10798-10802 (2015).
149 He, H. *et al.* Highly-efficient conversion of SF_6 via an eight-electron transfer process in lithium batteries. *Nano Energy*, 104679 (2020).
150 Braun, T., Noveski, D., Neumann, B. & Stammler, H. G. Conversion of hexafluoropropene into 1, 1, 1‐trifluoropropane by rhodium‐mediated C-F activation. *Angew. Chem., Int. Ed.* **41**, 2745-2748 (2002).
151 Zámostná, L. & Braun, T. Catalytic degradation of sulfur hexafluoride by rhodium complexes. *Angew. Chem., Int. Ed.* **55**, 15072–15075 (2015).
152 Gao, H., Li, Y., Guo, R. & Gallant, B. M. Controlling fluoride‐forming reactions for improved rate capability in lithium‐perfluorinated gas conversion batteries. *Adv. Energy Mater.*, 1900393 (2019).
153 He, M., Li, Y., Guo, R. & Gallant, B. M. Electrochemical conversion of nitrogen trifluoride as a gas-to-solid cathode in Li batteries. *J. Phys. Chem. Lett.* **9**, 4700-4706 (2018).
154 Ma, J.-L., Bao, D., Shi, M.-M., Yan, J.-M. & Zhang, X.-B. Reversible nitrogen fixation based on a rechargeable lithium-nitrogen battery for energy storage. *Chem* **2**, 525-532 (2017).
155 Parr, R. G. & Pearson, R. G. Absolute hardness: companion parameter to absolute electronegativity. *J. Am. Chem. Soc.* **105**, 7512-7516 (1983).
156 Pearson, R. G. Absolute electronegativity and hardness correlated with molecular orbital theory. *Proc. Natl. Acad. Sci.* **83**, 8440-8441 (1986).
157 Pearson, R. G. Hard and soft acids and bases. *J. Am. Chem. Soc.* **85**, 3533-3539 (1963).
158 Travers, M. J., Cowles, D. C. & Ellison, G. B. Reinvestigation of the electron affinities of O_2 and NO. *Chem. Phys. Lett.* **164**, 449-455 (1989).
159 Johnson III, R. D. *NIST computational chemistry comparison and benchmark database*. (NIST Standard Reference Database Number 101, 2019).
160 Sun, B. *et al.* Hierarchical porous carbon spheres for high‐performance Na‐O_2 batteries. *Adv. Mater.* **29**, 1606816 (2017).
161 Zhang, Z. *et al.* The first introduction of graphene to rechargeable Li–CO_2 batteries. *Angew. Chem., Int. Ed.* **54**, 6550-6553 (2015).
162 Xiao, N., Ren, X., He, M., McCulloch, W. D. & Wu, Y. Probing mechanisms for inverse correlation between rate performance and capacity in K–O_2 batteries. *ACS Appl. Mater. Interfaces* **9**, 4301-4308 (2017).

163 Tatara, R. *et al.* Oxygen reduction reaction in highly concentrated electrolyte solutions of lithium bis (trifluoromethanesulfonyl) amide/dimethyl sulfoxide. *J. Phys. Chem. C* **121**, 9162-9172 (2017).
164 Adams, B. D. *et al.* Current density dependence of peroxide formation in the Li–O_2 battery and its effect on charge. *Energy Environ. Sci.* **6**, 1772-1778 (2013).
165 Liu, Y., Wang, R., Lyu, Y., Li, H. & Chen, L. Rechargeable Li/CO_2–O_2 (2: 1) battery and Li/CO_2 battery. *Energy Environ. Sci.* **7**, 677-681 (2014).
166 Black, R., Lee, J. H., Adams, B., Mims, C. A. & Nazar, L. F. The role of catalysts and peroxide oxidation in lithium–oxygen batteries. *Angew. Chem., Int. Ed.* **52**, 392-396 (2013).
167 Li, J. & Rogachev, A. Y. SO_2–yet another two-faced ligand. *Phys. Chem. Chem. Phys.* **17**, 1987-2000 (2015).
168 Tang, R. & Callaway, J. Electronic structure of SF_6. *J. Chem. Phys.* **84**, 6854-6860 (1986).
169 McLean, A. Extended basis‐set LCSTO—MO—SCF calculations on the ground state of carbon dioxide. *J. Chem. Phys.* **38**, 1347-1355 (1963).
170 Jürgensen, A. & Cavell, R. G. Valence shell photoionization energies and cross-sections of NF_3 and PF_3. *J. Electron Spectrosc. Relat. Phenom.* **128**, 245-260 (2003).
171 Cade, P. E. & Wahl, A. C. Hartree-Fock-Roothaan wavefunctions for diatomic molecules: II. First-row homonuclear systems A_2, $A_2^{\pm}$, and A_2*. *At. Data Nucl. Data Tables* **13**, 339-389 (1974).
172 Jain, A. *et al.* The Materials Project: A materials genome approach to accelerating materials innovation. *APL Mater.* **1**, 011002 (2013).
173 Zintl, E., Harder, A. & Dauth, B. Gitterstruktur der oxyde, sulfide, selenide und telluride des lithiums, natriums und kaliums. *Z. Elektrochem.* **40**, 588-593 (1934).
174 Vannerberg, N. G. Peroxides, superoxides, and ozonides of the metals of groups Ia, IIa, and IIb. *Prog. Inorg. Chem.* **4** (1962).

Acknowledgments

The authors gratefully acknowledge funding from the MIT Lincoln Laboratory and from the Army Research Office under Award Number W911NF-19-1-0311.

Author contributions

All authors contributed equally to the preparation of this manuscript.

Competing interests statement

The authors declare no competing interests.

Display Items

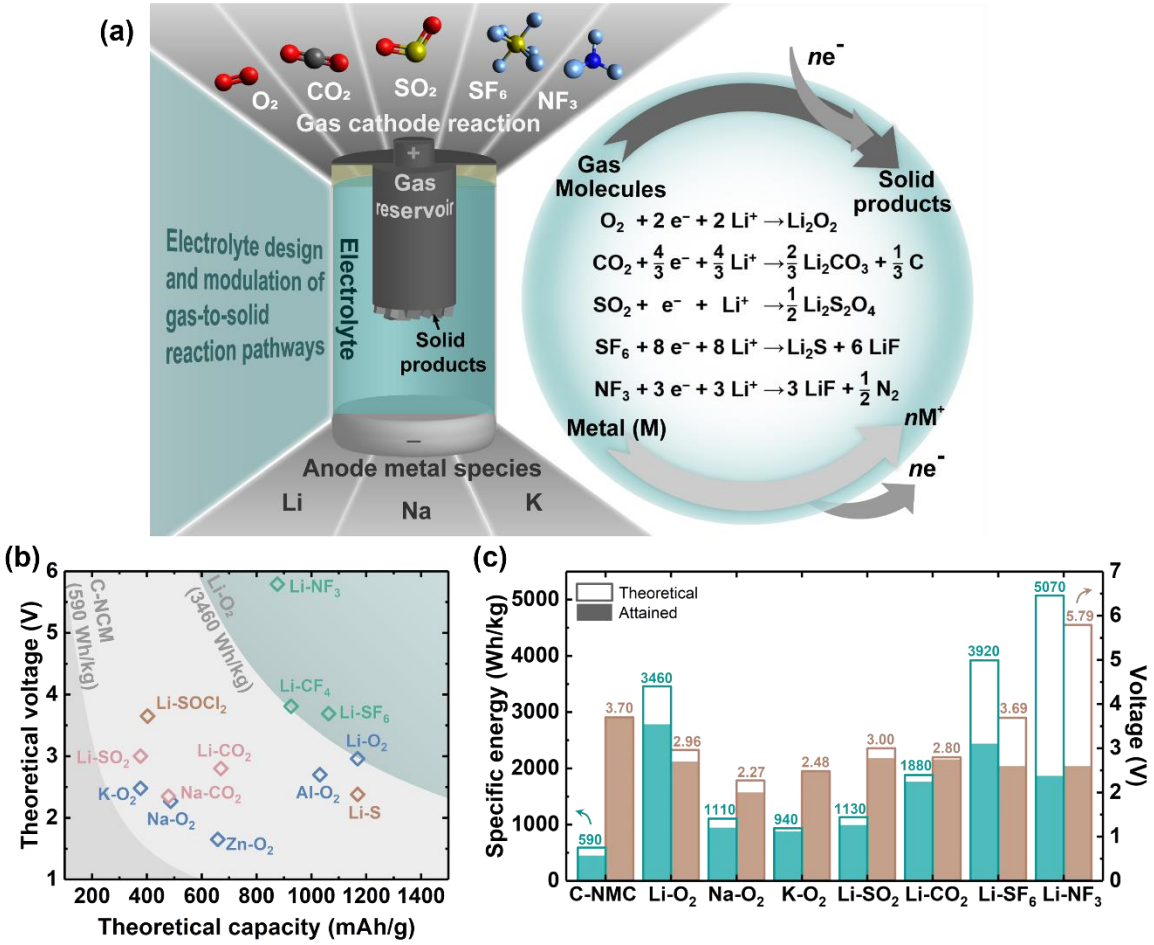

Fig. 1| **Promise and performance of nonaqueous metal−gas batteries. a** | Metal−gas batteries: Parameter landscape. Design variables include the metal anode, gas cathode, and electrolyte, particularly the solvent. **b** | Voltage−capacity metrics (theoretical) of different metal−gas battery couples including select non-alkali, aqueous anode candidates (Al, Zn) for comparison. The three shaded regions delineate specific energy ranges: lower than Li-ion (graphite−$LiNi_xMn_yCo_{1-x-y}O_2$, denoted C−NCM), higher than Li-ion but lower than Li−O_2, and higher than Li−O_2. **c** | Theoretical vs. attained specific energy (left axis) and voltage (right axis). The parameters are obtained from experiments using carbon cathodes (no catalyst) without electrolyte additives (see Supplementary Information for details). Part **c** was drawn using data from Refs 18 (Royal Society of Chemistry), 2 and 125 (Springer Nature), 152, 160 and 161 (Wiley-VCH), 153, 162 and 163 (American Chemical Society).

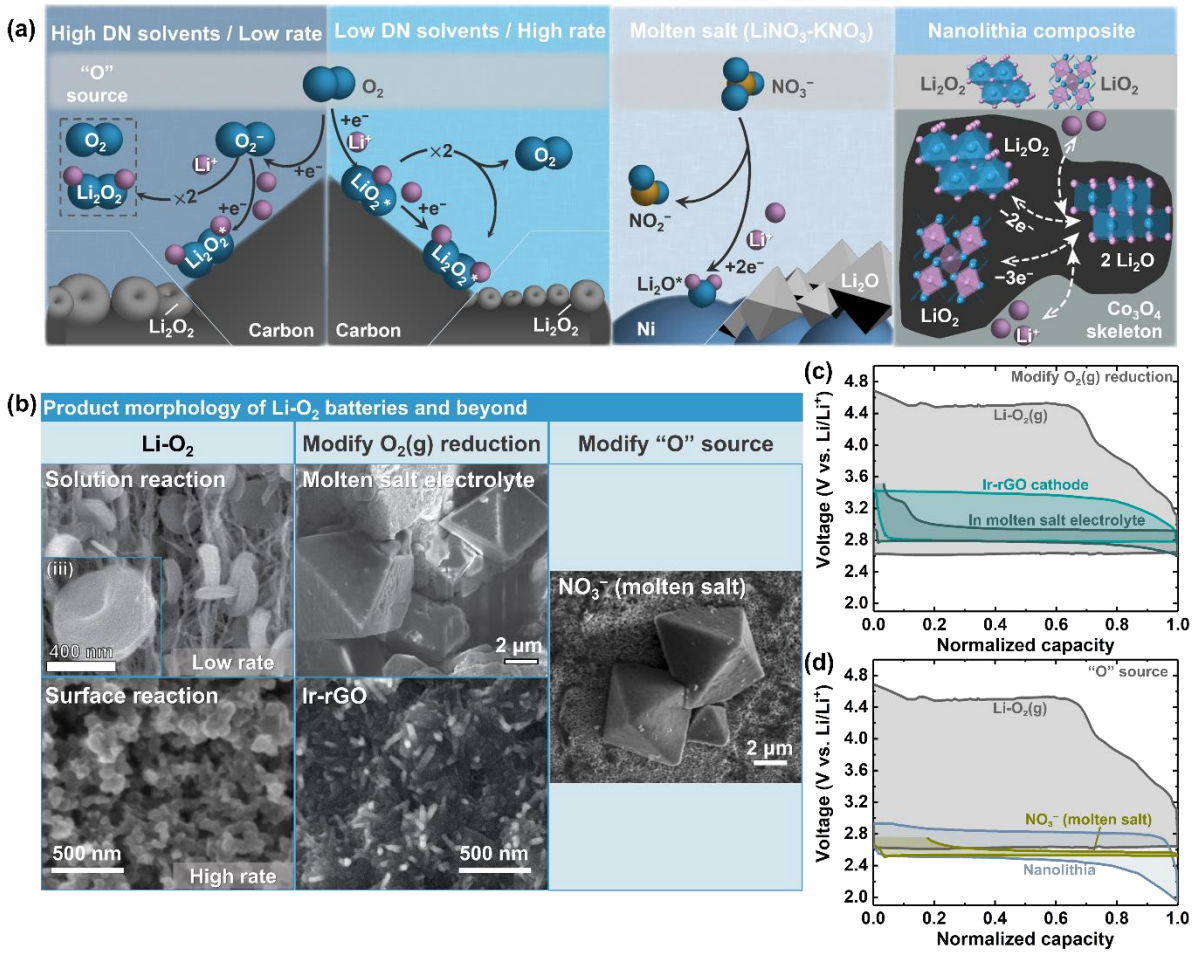

Fig. 2 | **Effect of electrolyte and 'O' source on nonaqueous Li−oxygen electrochemistry. a** | Schematic of three "O" sources in Li−oxygen batteries and their discharge mechanisms: O_2(g) (dissolved gas/solid), $LiNO_3$ (molten salt/solid), and Li_2O−Li_2O_2/LiO_2 (solid/solid). **b** | Morphology of solid products of Li−oxygen batteries, as indicated, obtained by Scanning Electron Microscopy. The inset in "solution reaction" was obtained at near-equilibrium growth conditions (10 mA/g_c). **c** | Galvanostatic cycle profile comparison for Li−O_2 with modified O_2(g) reduction pathways. **d** | Galvanostatic cycle profile comparison for Li−oxygen with different "O" sources (NO_3^-, nanolithia). See Table S3 for references and corresponding experimental details for **b**−**d**. Part **b** adapted with permission from Refs 164 (Royal Society of Chemistry), 22 (American Chemical Society), 84 and 89 (Springer Nature) and 88 (AAAS). Part **c** adapted with permission from Refs 30 (American Chemical Society), 84 (Springer Nature), and 88 (AAAS). Part **d** adapted with permission from Refs 30 (American Chemical Society), 89 and 92 (Springer Nature).

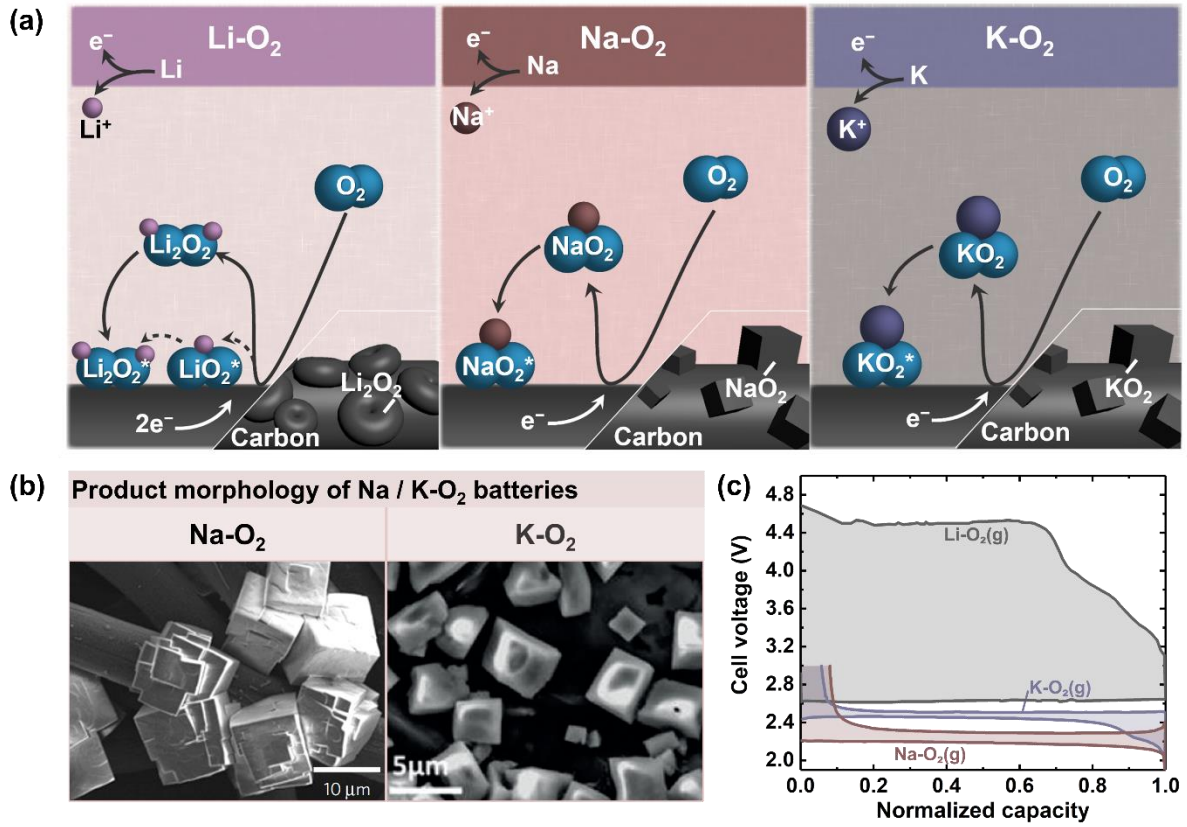

Fig. 3 | **The role of the alkali metal anode in unlocking reversibility. a** | Schematic depicting the discharge mechanisms of Li/Na/K−O_2 batteries (charging entails the reverse processes). For Li−O_2, dashed lines indicate the surface reaction pathway such as occurs in low-donor number (DN) solvents; the solution pathway (such as in high DN solvents) is indicated with solid lines. **b** | Morphology of discharge products in Na−O_2 and K−O_2 batteries by Scanning Electron Microscopy. **c** | Galvanostatic cycle profile comparison for the Li/Na/K−O_2 series. All cells used carbon paper as cathodes and were discharged/charged at an areal rate of ~ 100 μA/cm^2. See Table S3 for references and corresponding experimental details for **b**−**c**. Part **b** is adapted with permission from Refs 94 (Springer Nature), and 111 (Wiley-VCH). Part **c** is adapted with permission from Refs 30 (American Chemical Society), 94 (Springer Nature), and 111 (Wiley-VCH).

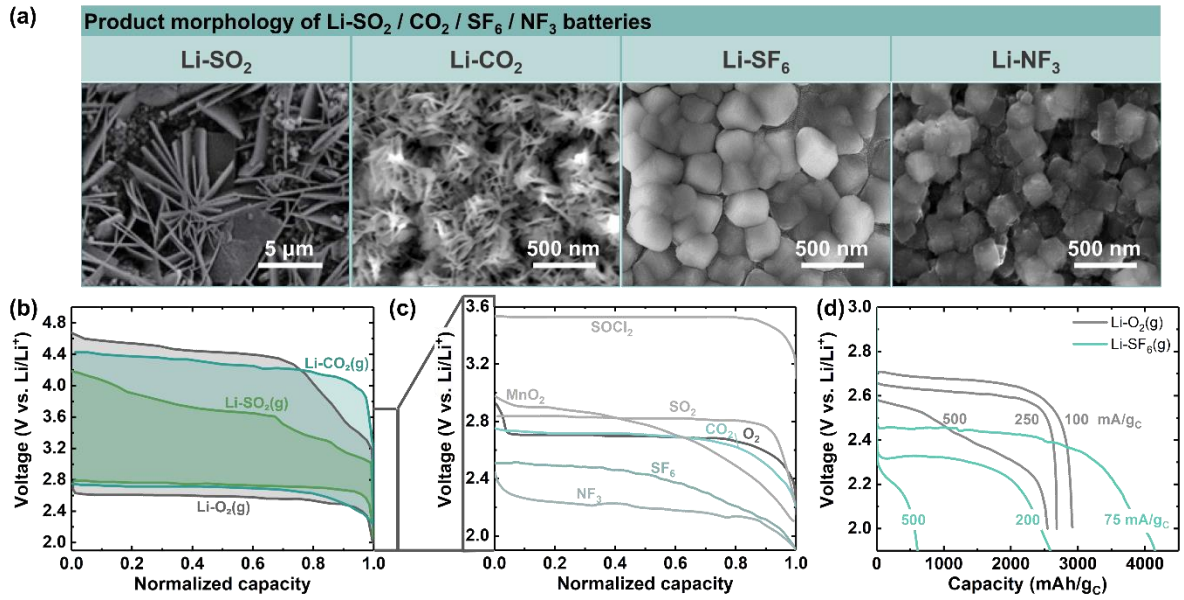

Fig. 4 | **Changing the gas cathode: Effects on morphology and electrochemistry**. **a** | Morphology of discharge products for Li−SO_2 / CO_2 / SF_6 / NF_3 gas cathodes (as indicated), obtained by Scanning Electron Microscopy. **b** | Experimental galvanostatic cycle profile comparison for Li−O_2, Li−SO_2, and Li−CO_2 batteries. All cells used Ketjen black (KB) carbon cathodes and were cycled at a rate of 0.2 mA/cm^2 (Li−O_2 and Li−SO_2) or 0.1 mA/cm^2 (Li−CO_2). **c** | Galvanostatic discharge curve of Li−O_2/CO_2/SF_6/NF_3 series compared with commercial Li-primary batteries: Li−$SOCl_2$(l), Li-SO_2(l), and Li-MnO_2(s). Cells for the Li−O_2/CO_2/SF_6/NF_3 series were discharged with KB cathodes at 140, 30, 30, and 20 mA/g_C, respectively. **d** | Rate capability comparison of Li−O_2 and Li−SF_6 batteries. Both cells were discharged with Vulcan carbon cathodes. See Table S3 for references and corresponding experimental details for **a**−**d**. Part **a** adapted with permission from Refs 125 (Springer Nature), 130 and 153 (American Chemical Society), 152 (Wiley-VCH). Part **b** adapted with permission from Refs 124 (Wiley-VCH), and 165 (Royal Society of Chemistry). Part **c** adapted with permission from Refs 166 (Wiley-VCH), 165 (Royal Society of Chemistry), 119 ((McGraw-Hill), 146 and 153 (American Chemical Society). Part **d** adapted with permission from Refs 152 (Wiley-VCH), and 20 (Royal Society of Chemistry).

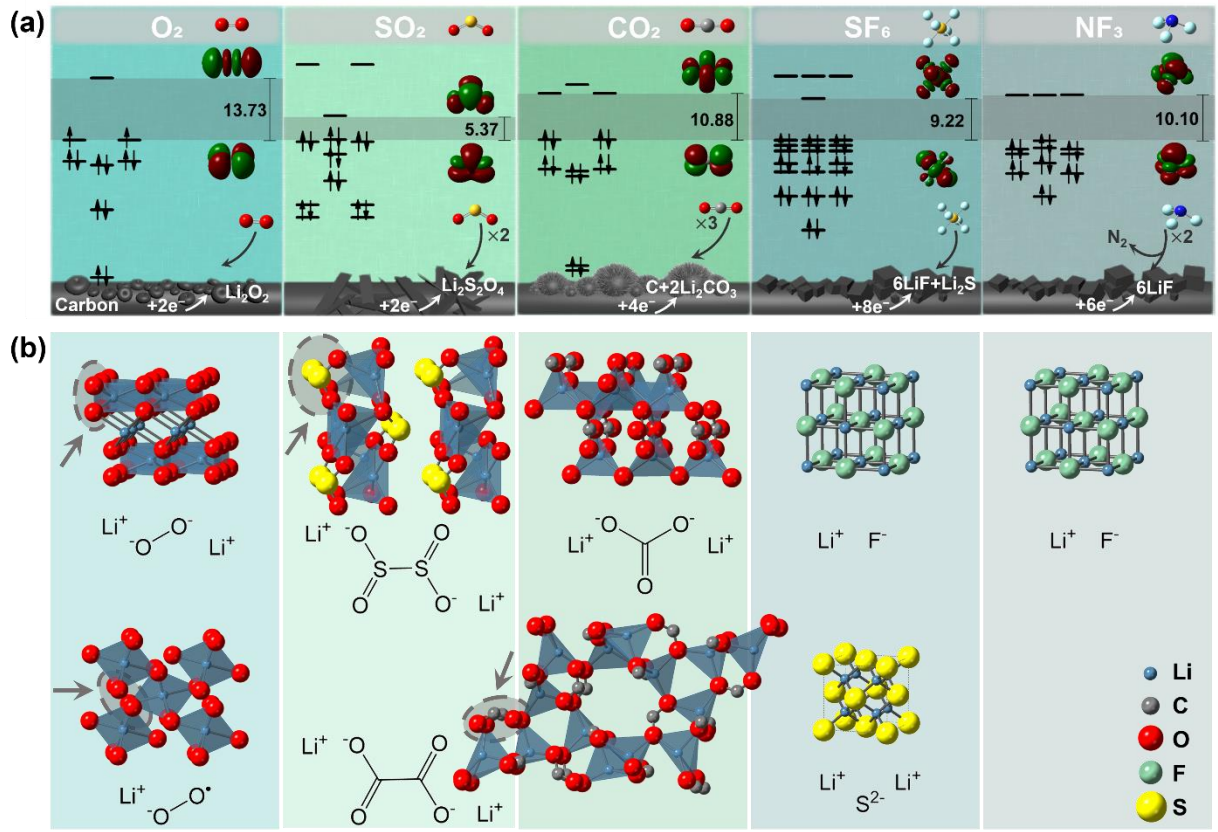

Fig. 5 | **Motifs underlying molecular and solid-state reversibility. a** | Comparison of reactant gas cathode molecules, including electronic structures: molecular orbital (MO) diagram; highest occupied MO (HOMO)−lowest unoccupied MO (LUMO) gap. The HOMO/LUMO gap energy were all obtained by DFT calculation using the B3LYP/6-31G** basis set. **b** | Lattice structure of Li_2O_2, Li_2CO_3, $Li_2C_2O_4$, $Li_2S_2O_4$ (adapted from $Na_2S_2O_4$), LiF and LiS. Circles/arrows indicate moieties within the solid phases (O-O pairing in Li_2O_2 and LiO_2, SO_2 motifs within $Li_2S_2O_4$, and CO_2 motifs within $Li_2C_2O_4$) predictive of reversibility. Note that LiO_2 is rarely observed as a stable discharge phase but is included here for comparison (similarly close O-O pairing is observed in the stable NaO_2 and KO_2 phases, Table 1). Likewise, $Li_2C_2O_4$ is not commonly observed in Li−CO_2 batteries where the primary product is the less-reversible Li_2CO_3, but is included here for comparison. Part **a** was drawn using data from Refs 159 (NIST), 167 (Royal Society of Chemistry), 168 and 169 (AIP), 170 and 171 (Elsevier). Part **b** was drawn using data from Refs 172 (AIP).

Table 1 | **Lattice structure data of alkali oxide phases (peroxide, superoxide, oxide)**. Key features are indicated: O-O bond length; alkali metal (Me)-O atomic distances;[173,174] Gibbs free energy of formation (from metal and O_2, per mole of alkali oxide); corresponding thermodynamic potential.[109]

Table 1 | Lattice structures and thermodynamic properties of alkali metal oxides, peroxides, and superoxides

Oxides	Lattice structure	Lattice constant (Å)	Bond-length (Å)		ΔG_r (kJ/mol)	E° (V)
			O-O	Me-O		
Li_2O	Antifluorite	a = 4.62	--	2.00	-561	2.91
Li_2O_2	Hexagonal	a = b = 3.12, c = 7.73	1.51	1.96−2.14	-570	2.96
LiO_2	Orthorhombic	a = 3.95, b = 4.94, c = 2.96	1.34	2.10	*	*
Na_2O	Antifluorite	a = 5.56	--	2.41	-376	1.95
Na_2O_2	Hexagonal	a = 6.21, c = 4.47	1.49	2.31−2.46	-449	2.33
NaO_2	FCC (disordered)	a = 5.49	1.33		-218	2.27
K_2O	Antifluorite	a = 6.45	--	2.79	-322	1.67
K_2O_2	Orthorhombic	a = 6.74, b = 7.00, c = 6.48	~1.5	2.66−2.74	-425	2.20
KO_2	Tetragonal	a = 5.70, c = 6.70	1.28	2.71−2.92	-239	2.48

* See discussion in Supplementary Information for the theoretical potential for LiO_2 formation.

ToC blurb

Demand for energy-dense electrochemical storage systems has drawn increasing focus to metal−gas batteries. This Review describes progress in the metal−gas family with a central focus on the underlying tension guiding evolution of the topic: tradeoffs in energy density vs. reversibility.